Addis Ababa institute of Technology
School of Graduate Studies
School of Mechanical and Industrial Engineering

Low Carbon Steel Characterization under Quasi-Static Strain Rate for Bumper Beam Application

A Thesis Submitted to the School of Graduate Studies of Addis Ababa institute of Technology in Partial Fulfillment of the Requirement for the Degree of Masters of Science in Mechanical Engineering (Mechanical Design)

Thesis by

Dawit Bogale Alemayehu

Advisor

Dr. Ermias Geberekidan

Addis Ababa University

Addis Ababa, Ethiopia

January, 2013

Low Carbon Steel Characterization under Quasi-Static Strain Rate for Bumper Beam Application

By

Dawit Bogale

Addis Ababa University institute of technology

Approved by board of examiners

_____	_____
Chairman	**Signature**
_____	_____
Advisor	**Signature**
_____	_____
Internal Examiner	**Signature**
_____	_____
External Examiner	**Signature**

January 2013

DECLARATION

Addis Ababa University
School of Graduate Studies

This is to certify that the thesis prepared by Dawit Bogale, entitled: Low Carbon Steel Characterization under Quasi-Static Strain Rate for Bumper Beam Application and submitted in partial fulfillment of the requirements for the degree of Master of Sciences (Mechanical Engineering: Mechanical Design) compiles with the regulations of the University and meets the accepted standards with respect to originality and quality.

Signed by the Examining Committee:

Department _____ Signature _____ Date _____

Advisor _____ Signature _____ Date _____

Chair of Department or Graduate Program Coordinator

ACKNOWLEDGEMENTS

Completion of this work would not have been possible without all help, all mercy, and his endless love the supernatural God Almighty. I express my deep sense of gratitude with sincere acknowledgements to my supervisor, Dr. Ermias Gebrekidan K for his invaluable guidance and encouragement throughout the study. I would also like to thank Walia Steel Industry and Metal and Engineering Corporation for making this research possible, and personally thank Mr. Sisay and Mr.Anteneh Gudisa staffs of Walia Steel Industry and Dr.Zewdu A, AAiT staff, for his many insights.

Last, I would like to thank my friend Messay Mekonene and Abiy Alene for their additional ideas for my research , and also Mr.Endalkachew for whom he guide me how to work on universal testing machine and teaching me how to use it safely and effectively.

I could able to produce this thesis because of the generous help of Dr. Daniel Tilahun R, who put his signature showing positive response in time of my Request letters whom I ask materials for my experimental purpose.

I am grateful to many laboratory technicians, including Zewede, Ayalsew, Yohannes, Kassay, Masresha and all the guys in the machine shop, without whom this work would not be completed. To my family, I cannot say enough. Thank you, my aunt misses. Tsedeku Alemayehu, for being my history whom show me to know my potential and to understand my internal potential. Because of you I am what I am today, Thank you.

I am grateful to my brother, Mr. Wondwossen Abubeker for his many advices during my stay in Addis Ababa and other friends who have always supported me.

Finally, I wish to dedicate this dissertation to my Grand mom Yesheye Wedneh whom she raised me from my child and my aunt Tsedeku Alemayehu and my father Bogale Alemayehu for their constant encouragement and all the pains they were through while bringing me up to this level.

Thank you! Dawit Bogale Alemayehu

ABSTRACT

Low Carbon Steel Characterization under Quasi-Static Strain rate For Bumper Beam Application

Dawit Bogale A

Addis Ababa University, 2013

This paper investigates the mechanical behavior of three selected steel materials which are considered to be the bulk material of front most bumper beam of a vehicle that is suddenly loaded in the quasi-static range. Thirty-six constant strain rate uniaxial tension tests were performed. The test was performed on a HUALONG Electro-hydraulic Universal testing machine at four strain rates ($3.33 \times 10^{-3}, 3.33 \times 10^{-2}, 3.33 \times 10^{-1}, 3.33\ s^{-1}$). The FEM which is ABAQUS/CAE is used to simulate the bumper subsystem using three low carbon steel. The outcome shows that UTS increase with an increase in strain rate and **HAS** material has the maximum mean UTS. The FEA in the post - processing stage gives the minimum displacement and maximum strain energy for **HAS** material when compared to the other two materials. Finally from both experimental and ABAQUS explicit analysis the result shows **HAS** material is better suit for the bumper beam application.

CONTENTS PAGE

LIST OF FIGURES

LIST OF TABLES

LIST OF SYMBOLS

Ao	Original cross-sectional area of specimen
lo	Original length of specimen
A	Cross-sectional area of specimen at fracture
σ_e	Engineering stress or laboratory stress
e	Engineering Strain or laboratory strain
Y	Yield Strength
F_{max}	Maximum applied load/force
ε	True strain
σ	Nominal stress
z or $\%\Delta l$	Percentage elongation
$\%RA$ or q	Percentage reduction in area
K	Strength Coefficient
n	Strain hardening exponent
σ^{-}	The yield stress at non zero strain rate
σ^0	The static yield stress
σy	Yield stress for JC material model
$\acute{\varepsilon}_0$	Reference strain rate
U, U1, U2, U3	Displacement Magnitude, in the X, Y and Z direction

E	Strain Components
E_{11}, E_{22}, E_{33}	Strain component in the X, Y, and Z direction
PE	Plastic Strain Components
PE_{11}, PE_{22}, PE_{33}, PE_{12}, PE_{13}, PE_{23}	Plastic strain components in the X,Y and Z direction and in XY, XZ and YZ Plane respectively
PEEQ	Equivalent Plastic Strain
PEEQMAX	Maximum equivalent Plastic strain through sectional
S	Stress component
S11, S22, S33, S12, S13, S23	Stress component in the X, Y, and Z direction and in the XY, XZ, and YZ plane respectively
V	Spatial Velocity
V1, V2, V3	Velocities in the X, Y, and Z direction respectively
A	Spatial Acceleration
A1, A2, and A3	Acceleration in the X, Y, and Z direction respectively
SE, ALLSE	Strain Energy and All Strain Energy
KE, ALLKE	Kinetic Energy and All Kinetic Energy
ETOTAL	Total Energy of the the output
UR, UR_1, UR_2, UR_3	Rotational Displacement
D^{el}	The Fourth-order Stress tensor
ε^{el}	total elastic strain (log strain in finite-strain problems)

LIST OF ABBREVIATIONS

SCS	Shear compression specimen
ULSAB	Ultra-light steel Auto Body
YS	Yield Stress
NHTSA	National High Way Traffic Safety Association
WSI	Walia Steel Industry
DDQ	Drawing Quality Steel
HSLA	High strength low Alloy Steel
DP	Dual Phase Steel
GTP	Growth and Transformation Plan
ASTM	American Standard Test Method
AISI	American Iron and Steel Institute
MTS	Material Testing System
SEA	Specific Energy Absorption
EA	Energy Absorption
AAiT	Addis Ababa institute of Technology
BC's	Boundary Conditions
FEM	Finite Element Method
FEA	Finite Element Analysis

CAE	Complete Abaqus Environment
CHs	Cross Head speed
UTS	Ultimate Tensile Strength
SDEV	Standard Deviation the given population for excel
AVE	Mean of the population data in excel

CHAPTER ONE

1. Introduction

1.1 Background

Steel is a material used to build the foundations of society. It is an iron-based material containing low amount of carbon and alloying elements that can be made into thousands of compounds with exciting properties to meet a wide range of engineering application. Steel is truly a versatile material. The value of steel produced annually is estimated over 400 billion USD. Thus steel finds its way into the world economy.

Nowadays, need of steels is soar up due to newly introduced massive construction projects in civil, mechanical, naval, aeronautical engineering and in other engineering fields. Particularly in developing countries, such as in Ethiopia, India, and china, steel materials are used extensively to develop infrastructure such as road, power, water, and telecommunication. According to the Ethiopian government Growth and Transformation Plan (GTP, 2010/11-2014/15), expansion and maintenance of infrastructures have been given high priority from the stand point of improve and sustaining pro-poor growth through job creation, initiating domestic industrial development in so doing contribute for poverty eradication effort of the country. In order to get this goal, adequate and reliable steel products should be produced and supplied to the end users.

In structural designs behaviors should be predictable and known at some level under different load and environment conditions to obtain safe and reliable designed systems. In this regard, one of critical issues during design stage and service life is dynamic response of steel materials. Their responses are dependent of several factors such as material source, type of productions (hot

working or cold working), heat treatment types, and application areas. Therefore, it is necessary for designers to understand the dynamic behavior of steel materials.

Recently, considerable attention has been given to the use of steel materials in construction sectors to understand their mechanical and thermo-mechanical behavior under different circumstances. This initiation mainly came from collapse of the two world trade center buildings which were attacked in Sep, 2001 by terrorist. Most of the literatures have concentrated on high–strain rate due to airplane impact and fire impact on the building materials [21].

To understand the performance of currently available selected construction steel materials under impact load, in this paper experimental and numerical method are considered. Specifically, product of Walia steel industry and Metal and Engineering Corporation are being chosen. The author beliefs that considering WSI's products are worth taking and it might represent the quality and performance of steel profiles.

The study concerns the effect of strain rates caused by dynamically loaded with impacts in the range of ($3.3*10^{-3}$ to $3.3s^{-1}$) or quisi-static and fire impacts. But the thermal effect (at elevated temperature) is not considered here because the tensile test has been takes place at room temperature. Therefore, the final aim is to increase the strength of this steel products to overcome slow speed impact by absorption of energy through deformation modeling (characterizing) it using numerical and experimental work. And also descriptions of permanent plastic deformations that are designed deliberately in a wide range of industrial processes like automobile industry for this paper, or occur accidentally under undesired overloads. The ABAQUS/CAE software (finite element method) is used to perform reliable simulations of impact experiments that produce plastic deformation in the selected steel specimen from the steel industries in Ethiopia. The numerical model accounts for the actual experimental setup used in the experiments, including testing of the selected items at different strain rate and tensile deformation using universal testing machine performed at room temperature. For the application part the from the car safety part the bumper subsystem is modeled using catia software and exported to ABAQUS/CAE in order to study the effect of strain rate during slow speed impact. Energy absorption from ABAQUS/CAE is compared observed and analyzed as well as the displacement.

1.2. Motivation

In Ethiopia automotive assembly, the technology itself is emerging and it opens several opportunities for the coming automobile industry. One of those opportunities is use of different materials for primary vehicle structures and the safety component. In this regard, steel materials are chosen because of their proffered mechanical properties, easy of availability and suitable for current automated production process in automotive industry.

Particularly, several body builder have been established in the past two decades to cop up with increasing demand of transport means due to unprecedented infrastructures expansion, rapid business developments and desire of high public transport. To fulfill this demand, production and supply of sufficient engineering materials are unquestionable. As a preliminary survey indicates that most vehicle bodies, truck and bus, are constructed using different types of mild steel structural and the main raw materials has been taken to construct vehicle body.

But the industry in Ethiopia in which the sample material is taken from for this study is Metal and Engineering Corporation is an industry with vast manufacturing, spare parts and assembly duties among this car assembly is one of the duties takes place. But the parts to be assembled are not manufactured here rather imported from other car manufacturing industry outside Ethiopia among this China. The city bus or locally called Beshoftu Bus is assembled here in Ethiopia in the above mentioned industry. The main motivation for this study is no awareness or attentions is given for crashworthiness there by the material for the safety part (Bumper beam) of the car is not tested weather the material is suitable for the intended application i.e. used as safety component to prevent the passengers from accidents during impact by other car or against rigid walls by absorbing impact energy. So this experiment plays crucial role for the automotive industry in Ethiopia by giving wakeup alarm to give attention for the design and manufacturing of the bumper beam in their own workshop.

1.3. Objectives of the study

The objective of this study is:-

1.3.1. General Objectives

The general objective of this thesis will cover demonstrating of the WSI and Metal and Engineering Corporation sample products for mechanical behavior under specified strain – rate and room temperature weather or not the products are consistent to the specification they were supplied. To select proper steel material for the car bumper beam using Experimental testing and using the result as input to finite element software like ABAQUS/CAE for impact simulation. And to give some awareness on crashworthiness and passenger safety to the above mentioned automobile industry found in Ethiopia. And also illustrate the effectiveness of numerical modeling method to represent the experimental model.

1.3.2. Specific objectives

The specific objectives of this paper are:

- To predict maximum deformation and energy absorption of the individual sample material there by selecting the best suit for the bumper application
- To study one of FEM software ABAQUS CAE and to implement for this study in order to construct each part, assemble and simulate for slow speed car impact
- Characterizing the sample specimens using special testing machine called servo electrohydraulic universal testing machine: testing the specimen for tensile load, recording the output variables and processing it on the spread sheet and analyzing the results
- To propose suitable steel material for the bumper beam
- Developing experimental design model and numerical (Mathematical and ABAQUS/CAE software) to characterize the behavior of selected steel profiles under dynamic and static loading condition.
- Study the effect of quasi-static strain rate on the selected material without considering thermal effect.

1.4. Scope of the project

This paper is confined to the following simple aspects and they are as follows:

- Literature study on steel characterizing and steel car bumper beam
- Observing carefully, Learning and exploring in a way to use Universal testing Machine
- Studying the FEM (ABAQUS/CAE) software in deep
- Implementing the knowledge of ABAQUS/CAE to simulate the model for slow speed impact
- Proposing a suitable low carbon steel material for commercial front bumper beam

2. Literature Review

Steel characterizing under Quasi-static strain rate for car Bumper Beam application both with numerical and experimental method is introduced in this paper. many scholars have wrote steel characterizing under different strain rates by employing different types of devices and modeling and simulating software's.

2.1. Materials characterization

[27], in their work, introduce the mechanical properties and microstructures of AISI 4340 high strength alloy steel under different tempering conditions are investigated. They also believe that an understanding of the mechanical properties of metals during deformation over a wide range of loading conditions is of considerable importance for a number of engineering applications. It has been reported that the superiority of super austenitic stainless steel, 254 SMO (S31254), lies in its high strength, good weldability and great resistance to stress corrosion and pitting because of its higher content of alloying chromium and molybdenum compared to general stainless steel. [7]**,** furthermore, the purpose of this paper is to investigate the effect of strain rate on the mechanical properties and microstructure variation of the super-austenitic stainless steel 254 SMO. The development of physically-based dislocation models of a mechanical response of materials under different strain rates and temperatures is an important problem of modern mechanics. If the microstructure is not affected much by changes in the strain rate and temperature, the models can be employed for predicting mechanical properties of pure metals and alloys under uniaxial loading conditions where in the specimen experiences isotropic homogeneous deformation up to the point of failure solely due to the motion of uniformly distributed defects (dislocations) [8]. Presented in this paper are the computational results on deformation of austenitic steels at different strain rates and temperatures.

Large strain mechanical behavior of 1018 Cold-Rolled Steel over a wide range of strain rates, the determination of large strain constitutive behavior of materials is a key step toward accurate modeling of numerous processes such as plastic forming, plastic fracture, and high-speed

penetration [15]. Here also other paper present, plastic deformation of 0.25" thick Ti-6Al-4V plate is investigated. Moreover, experimental data for plastic deformation of Ti-6Al-4V (from hereafter, referred to as Ti64) is generated and studied over a vast range of strain rates, in different directions of the metal alloy plate and at various temperatures [21].

[22], investigated in his paper, Post impact strain measurements of damaged plates were carried out experimentally after launching a spherical steel projectile at varying velocities against a fixed thin plate targets made of copper and steel materials and constrained at their outer periphery. The data obtained for high strain rates could be very valuable for the design of trauma plates in bullet proof vests, aircraft and missile impact on structures and buildings including nuclear power plants, crashworthiness of automotive systems, and space debris impact on space structures placed in orbits. Here in the present project, three different steel materials are tested under tension experimentally and the data obtained from the experiment is used for the application of the bumper beam (crashworthiness of automotive systems) material which is the bulk material in question [13]. This report provides five types of mechanical properties for steels from the World Trade Center (WTC): elastic, room-temperature tensile, room-temperature high strain rate, impact, and elevated-temperature tensile. Specimens of 29 different steels representing the 12 identified strength levels in the building as built were characterized. Elastic properties include modulus, E, and Poisson's ratio, ν, for temperatures up to 900 °C. The expression for E(T) for T<723 °C is based on measurements of WTC perimeter column steels. Behavior for T>723 °C is estimated from literature data. Room temperature tensile properties include yield and tensile strength and total elongation for samples of all grades of steel used in the towers. The report provides model stress-strain curves for each type of steel, estimated from the measured stress-strain curves, surviving mill test reports, and historically expected values. With a few exceptions, the recovered steels, bolts, and welds met the specifications they were supplied to. Here the report shows that the world trade center steels are characterized under different strain rate and different temperatures to relate to apply for the real airplane impact and also to overcome the fire impact which is the major research question of the present paper but the application is different and also the strain rate range is intermediate and most importantly in this present paper temperature other than room temperature is not considered. Also other research is presented by [25]the research has considered the characterization of the high strain rate constitutive response

of three steels: a drawing quality steel (DDQ), a high strength low alloy steel (HSLA350), and a dual phase steel (DP600).

The automobile industry has been improved significantly since 1953 by emerging the composite materials [10]. Since it is proved that the composite materials can achieve the desirable properties such as low weight, high fatigue strength, easy forming and high strength, they are suitable for material replacing. Although the composites have some undesirable properties such as relatively long time processing, expensive raw materials and low surface finish quality, its light weight is the major reason for the increasing application of the composite materials in the automobile industry. Whereas [1]found that the vast majority of bumper reinforcement systems today are made from steel. Steel beams have a low unit material cost, and have a greater strength to weight ratio than most aluminum beams and composite material beams.

Another paper analyzes the impact behavior of a composite car bumper made from new materials. The study is performed using Solid works software for the design of the new car bumper made from new composite materials and the stress concentration distribution is evaluated by use of finite element analyze with Abaqus software for the impact cases. The first objective it provides important information about each car safety rating as a score. The second objective it provides important data to producers for safety improvements. Some examples of their tests are: frontal, side, pole impact and children, pedestrian protection. [7] and they also stated that the automotive industry is concerned based on development of primary car safety equipments. This study focuses in the application of new composite materials in a front car bumper. The author of this paper also agrees with the debate stated above because car Bumper as safety component is not realized in Ethiopia although there are car assembly industries like Metal and Engineering Corporation. This industry is one of known metal processing industries in Ethiopia most importantly recently it started assembling of city bus known by Beshoftu bus. But here there is no any awareness of crashworthiness concept or safety related to car impact at slow speed. The WSI is steel industry that process it and sale for customers.one objective of this paper is to make awareness and give some clue for the automotive industry emerging in Ethiopia further to give attention for the crash worthiness to fulfill this achievement this paper play a crucial role through selection of proper steel material for the bumper considering weight reduction and fuel consumption also energy absorption as major criteria.

2.2. Strain rate range and its effect

One of the defining features of impacts that occur at velocities sufficiently large to cause inelastic (and particularly plastic) deformations is that most of these deformations occur at high strain-rates. These deformations may also lead to large strains and high temperatures. Unfortunately, we do not understand the high-strain-rate behavior of many materials (often de-fined as the dependence $\sigma_f(\varepsilon, \dot{\varepsilon}, T)$ of the flow stress on the strain, strain rate and temperature), and this is particularly true at high strains and high temperatures. A number of experimental techniques have therefore been developed to measure the properties of materials at high strain-rates. In this section we focus on those experimental techniques that develop controlled high rates of deformation in the bulk of the specimen, rather than those in which high-strain-rates are developed just behind a propagating wave front [25].

The primary experimental techniques associated with the measurement of the rate dependent properties of materials are described in Fig 1 (note that the stress states developed within the various techniques are not necessarily identical). An excellent and relatively recent review of these methods is presented by [11]. For the purposes of this discussion, strain rates above 10^2 s^{-1} are classified as high strain rates, strain rates above 10^4 s^{-1} are called very high strain rates, and strain rates above 10^6 s^{-1} are called ultra-high strain rates. Conventionally, strain rates at or below 10^{-3} s^{-1} are considered to represent quasi-static deformations, and strain rates below 10^{-6} s^{-1} are considered to be in the creep domain. Creep experiments are typically performed at relatively high temperatures and a variety of specialized machines exist for these kinds of loading; dead loads are often of particular interest. Quasi static experiments are typically accomplished through a variety of servo hydraulic machines, and ASTM standards exist for most of these experiments. Most servo-hydraulic ma-chines are unable to develop strain rates larger than 10^0 s^{-1} repeatably, but some specialized servo-hydraulic machines can achieve strain rates of 10^1 s^{-1}. Finally, the strain rates in the intermediate rate domain (between 10^0 s^{-1} and 10^2 s^{-1}) are extremely difficult to study, since this is a domain in which wave-propagation is relevant and cannot be easily accounted for (how-ever, the strain rates in this domain are indeed of interest to a number of machining problems). The primary approach to testing in this strain rate range uses drop towers or drop weight machines [9], and great care must be exercised in interpreting the data because of the coupling between impact-induced wave propagation and machine vibrations.

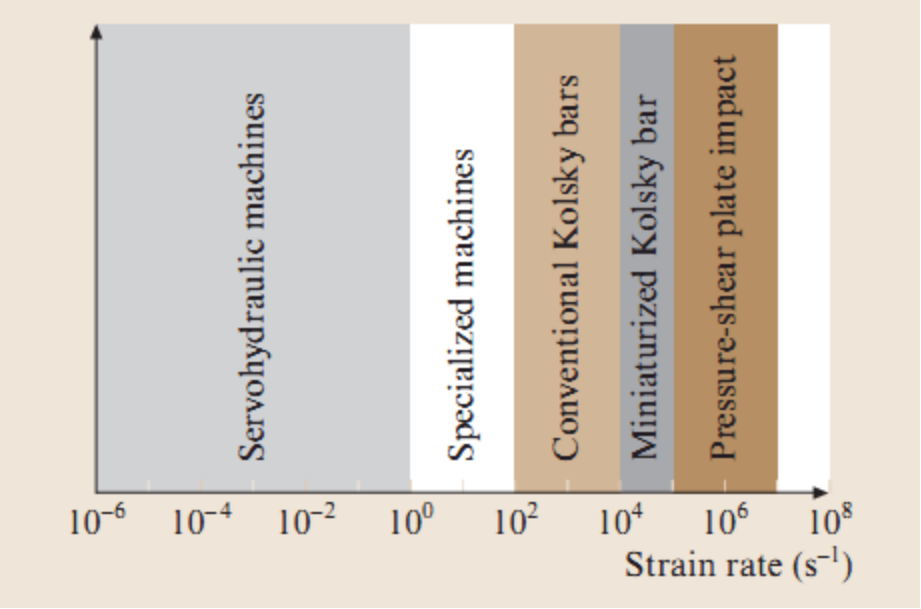

Figure 1 Experimental techniques used for the development of controlled high strain rate deformations in materials [9].

More recently, consideration was given to the impact of the rate of straining of a particular material or component on its performance. Since steel is a strain rate sensitive material, its yield strength increases as the loading rate increases. This provides further benefits in its ability to sustain and absorb higher loads and higher input energy, such as in the case of deformation of a bumper or other structural component. Again, this is not a new discovery but it was only through the introduction of the advanced vehicle concepts phase of the ULSAB (Ultra-Light Steel Auto Body) development that this benefit of steel began to be introduced in structural design of automobile components. Considerable effort was then expended in various laboratories around the world to generate tensile data at straining rates ranging from quasi-static (10^{-3} s^{-1}) to 10^{3} s^{-1} for many of the above steel grades [3].

In the study of [15], the strain rate is the main factor to characterize the material under study. Here the large-strain constitutive behavior of cold-rolled 1018 steel has been characterized at strain rates ranging from 10^{-3} to10^{4} s^{-1} using a newly developed shear compression specimen (SCS). Where as in other research strain rate rage is taken on the base of experimental data on uniaxial loading of new steels in the range of strain rates from 0.001 to 500 s^{-1} the model parameters were derived, and dynamic responses of the steels were predicted, within the range of strain rates up to 8000 s^{-1} [18]. Another paper which is has the same objective with this present

research present is the quasi-static strain ranges which is the tensile test s were performed at four strain rates: 1×10^{-1}, 1×10^{-2}, 1×10^{-3} and $1 \times 10^{-4} s^{-1}$. In this range the effect of the strain rate is also stated as follows ductility vs. strain rate violates the normal condition that the elongation reduces as the strain rate increases. For example, the elongation would be 33% at a strain rate of $1 \times 10^{-1} s^{-1}$, but 25% at a strain rate of $1 \times 10^{-4} s^{-1}$. In the meantime, more shear bands formed in the grain at the high strain rate of 1×10^{-1} s^{-1} than at the low strain rate of $1 \times 10^{-4} s^{-1}$ [7]. Also it is found that the longer flat-top strain and higher work-hardening rate occur at the higher strain rate and the summarized ultimate tensile strength (UTS) and the yield strength (YS), which shows that these strengths are not strongly influenced by the variation of strain rate. The average YS is about 430 MPa and the average UTS is about 750 MPa. On the contrary, the total elongation is conspicuously higher with strain rate increases. The reduction in area is also reduced with increasing strain rate as shown below in the table.

Table 1 The value of the reduction area (RA %) and the strain-hardening exponent

Strain rate (s^{-1})	*RA%*	*n*
1×10^{-1}	*66.8*	*0.29*
1×10^{-2}	*58.6*	*0.26*
1×10^{-3}	*53*	*0.25*
1×10^{-4}	*52.3*	*0.24*

[27], here the author consider constant strain rate which is in the range of quasi-static. In this work the specimens are quenched and tempered to a martensite structure and loaded to fracture at a constant strain-rate of 3.3×10^{-4} s^{-1} by means of a dynamic material testing machine (MTS 810). The size and geometry of the specimens as well as the testing procedure are in accordance with ASTM standard E 8 (1981) for tension testing. Under this standard a nominal gauge length of 50 mm and a gauge of 12.5 mm are utilized in preparing the specimens and this present work also uses this standard so that the same specimen size but the specimen are tested in the quasi-static ranges taking four strain rate range to investigate the effect of the strain rate . For mechanical tests, the specimens are mounted on a dynamic material testing system (MTS) and

pulled to fracture at room temperature with a constant cross-head speed of 0.0083 mm s1, which corresponds to an initial strain rate of 3.3×10^{-4} s^{-1} (if all the crosshead movement is transmitted to the specimen), in order to obtain the room temperature flow properties. And this research agree with the present work that it uses the mechanical properties, such as ultimate tensile strength, yield strength, and percentage reduction area, are calculated from the stress – strain diagrams obtained from the tensile testing, in which the latter three specimens under identical conditions are used. In this study it also considers the strain hardening exponent which very important parameters in mechanical behavior of a material from the true stress – strain curves for AISI 4340 steel conform closely to Ludwik's relationships

$$\boldsymbol{\sigma = K\varepsilon^{n}} \qquad \textit{Equation 1}$$

where K is the strength coefficient and n is the strain-hardening exponent. These two constants describe completely the shape of the true stress – strain curves. The value of 'K' provides some indication of the level of strength of the material and of the magnitude of forces required in forming, whilst the value of 'n' correlates the slope of the true stress – strain curve, i.e. the rate of work hardening, which provides a measure of the ability of the material to retard localization of deformation. In uniaxial tension, the equivalent stress σ_i equals the tensile stress σ, and the equivalent strain ε_i equals the tensile strain ε, consequently the true stress – strain curve is the same as the curve $\sigma=K\varepsilon^n$. The stress σ must not be greater than the tensile instability stress σ_{crit} which corresponds to the maximum load in simple tension and in turn marks the end of uniform straining, thus $\sigma_{crit} =K(\varepsilon_{crit})^n$. [21]**,** this is another unique work on Plastic deformation of 0.25" thick Ti-6Al-4V plate is investigated. Compression, tension and shear tests are carried out from quasi static strain rates (10^{-4} s^{-1}, 10^{-2} s^{-1}) to high strain rates (up to $5x10^3$ s^{-1}) to study the strain rate sensitivity of the material. Tension and compression tests are carried out on specimens machined in different directions of the plate (at 0°, ±45°, 90° to the rolling direction of the plate in tension and at 0°, ±45°, 90° to the rolling direction and through the thickness of the plate for compression tests) to study the anisotropy effects. Also other part of the work explains techniques and experimental setups used for the quasi-static and low strain rate testing of Ti64. An INSTRON 1321 model biaxial servo hydraulic testing machine has been used to test Ti64 for all of slow rate compression, tension and torsion tests. Figure1. Shows the servo hydraulic machine with the important components indicated on the figure below and the machine can move ±2.41" (61.214mm) and can rotate ±45° about the vertical axis. The load frame can

accommodate two load cells, a Lebow-6467-107 cell with thrust capacity 20,000 lb (88.96 kN) and 10,000 in.lb (1129.85 Nm) torque capacity and a Load cell Grips holding Push rods DIC Cameras Push rods Specimen 37smaller Interface 1216CEW-2K with 2,000 lb (8.896 kN) thrust capacity and 1000 in.lb (112.99 Nm) torque capacity. The smaller cell is used in experiments which incur small loads/torques for greater accuracy of the load/torque data. The machine is controlled with a MTS Flex Test SE controller through multi-purpose software. It can capture data at up to 100 kHz through MTS 493.25 digital signal conditioner. Simple procedure of step by step instructions can be written in the software to repeat similar tests. Quasi static tests were performed at three strain rates viz. 10^{-4} s^{-1} , 10^{-2} s^{-1} and $1s^{-1}$ (100 s^{-1}) in all compression, tension and shear loading.

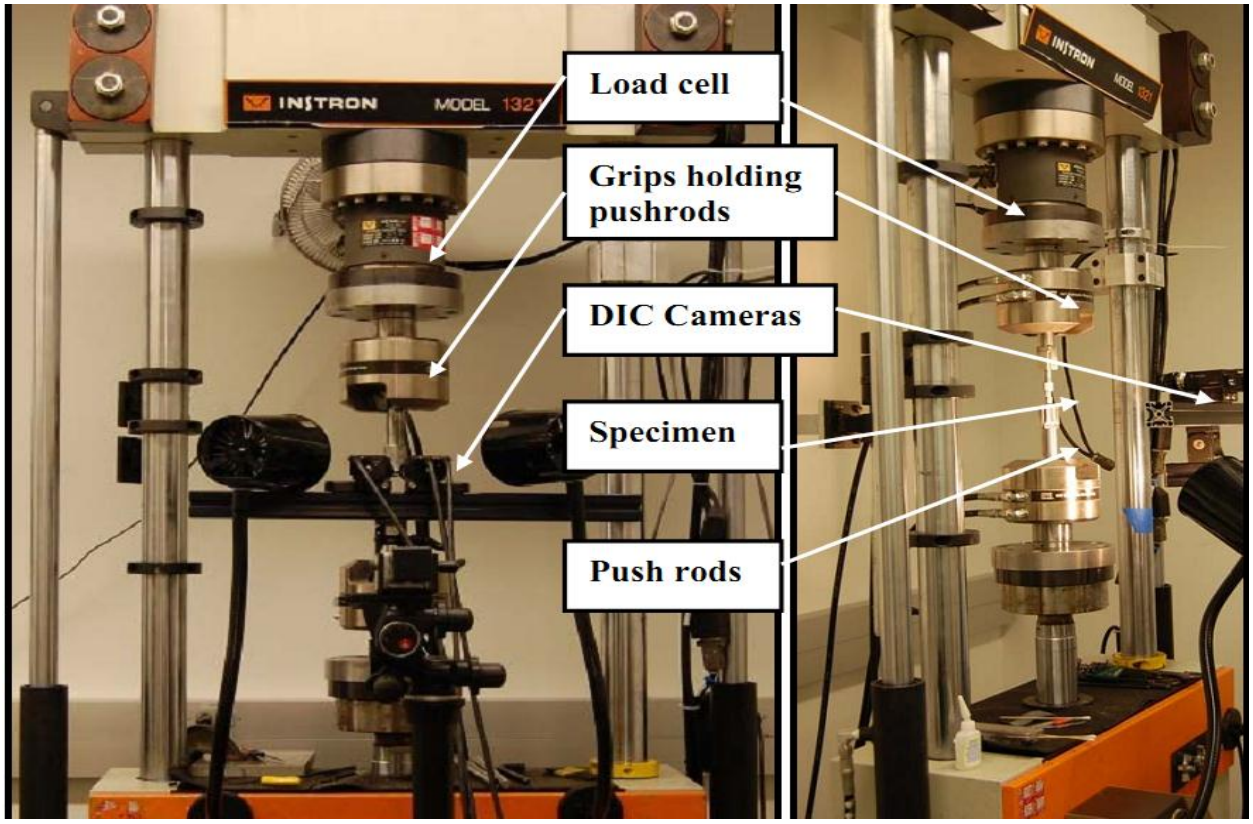

Figure 2 Instron machine with the digital image correlation setup at the Dynamic Mechanics of Materials Laboratory, OSU, a) Front view b) Side view[22].

The strain rate sensitivity study of this work shows that the strain rate sensitivity of the material Ti-6Al-4V is illustrated in these plots as the yield stress increases with increase in strain rate

from 10^{-4} s^{-1} to 10^{3} s^{-1} in all loading modes. It can also be seen that the rate of strain hardening of the material changes with strain rate i.e. at lower strain rate a steeper post yield stress strain curve is observed as compared to a flatter post yield curve observed at higher strain rates. whereas other investigation by [22]**,** his work was on Post impact strain measurements of damaged plates were carried out experimentally after launching a spherical steel projectile at varying velocities against a fixed thin plate targets made of copper and steel materials and constrained at their outer periphery. This research is done under strain rates achieved during the experiments varied from 8000s^{-1} to 15000 $s^{-1}$for steel specimens and from 9000 $s^{-1}$to 19000 $s^{-1}$for copper specimens for the projectile speeds of 68 to 120 m/s. Since the experiment is performed at high strain rate for both steel and copper material it is their difference with the present work is far apart. But here their common objective is that both of the works study the different range of strain rate effect on materials during impact**.** A study by [14], is another paper which is an investigation that takes place in United State of America one of unforgettable accident on the twins WTC which is attacked by terrorist by high impact aircraft. So the material that lefts from the attack are investigated through experiment and mill test to know the mechanical properties. An important additive correction to the estimated yield strength is necessary because the experimental and mill test report values are enhanced because the tests are not conducted at zero strain rate. Properly, the yield strength in a mill test report or experimental determination is dynamic yield strength, σ_{yd}. For modeling building performance, the appropriate strength is the static, or zero strain rates, yield strength σ_{ys}. Starting from the static yield strength, all the strength enhancements due to strain rate effects, such as produced in the aircraft impact, can be calculated. From tests on several different structural steels, [20] estimated that for strain rates, $16\times10^{-4}s^{-}1 > \acute{\varepsilon} > 2\times10^{-4}s^{-1}$, the difference between and static, σ_{ys}, and dynamic σ_{yd}, yield strength can be represented by

$$\sigma_{ys} - \sigma_{yd} = -(3.2 - 1000\acute{\varepsilon}) = K_{dynamic} \qquad \textit{Equation 2}$$

It is well known that the yield and ultimate strengths of steels increase with increasing strain rate . In terms of the mechanical response of the steels in the towers, the high-speed impact of the aircraft is a high-strain-rate event, which is well above the conventional strain rates normally associated with mechanical properties measurements. It is estimated that the strain rates on the World Trade Center (WTC) steels, due to the aircraft impacts, were up to 1000 s^{-1}. Accurate

models of the aircraft impact and the resulting damage to the towers require knowledge of the mechanical properties of the steels at high strain rates. There is a gap between the present paper and this study that is in this present paper the impact under study is slow speed impact, the secondly the application is on the car beam bumper unlike the WTC study which is concentrates on the building materials like bolts, column bars, and etc. which left from the destruction of the building, and thirdly the strain rate range is quasi-static for the present paper but for this literature it is under high strain rate because the aircraft hit the building at high speed or at high speed impact. The other difference is the literature of the WTC material investigation for their mechanical behavior is they consider importantly the effect of temperature because there were fire after the building is impacted by the high speed aircrafts. Here the high-temperature testing program had two thrusts. One was to characterize the elevated-temperature stress-strain behavior of the steels most likely to have been affected by the post-impact fires. The second was to characterize the creep, or time-dependent deformation, behavior of the steels from the floor trusses. In each of these two areas, in addition to the experimental characterization, NIST developed methodologies to predict the behavior of untested steels. But in this present research there are no devices available to investigate the behavior of the three sample plain low carbon steel their behavior at elevated temperature. [23] Here also the effect and strain rate range is discussed in this work that the variation in material strength with applied strain rate is an important consideration in the design of classes of materials used in structures subjected to suddenly applied loads. It has been observed that for many materials the stress is found to increase rapidly with strain rate for a given suddenly applied load. This effect is shown in Figure 2, which shows schematically the threshold value at which such changes are observed as related to a particular material type and specified dynamic load. Generally, such changes are observed to occur at strain rates of the order of magnitude 30/sec for metals. This paper also tries to discuss the ranges of strain rate under different loading condition. For strain rates exceeding 1/sec, which can be considered as an initial starting point for evaluating dynamic load effects as related to material rate sensitivity, the following types of tests have been used:

In order to understand this behavior and gain insight into the development of suitable mathematical models for describing the behavior of materials at high strain rates, a number of important issues are needed. Among these issues are·

- ✓ Direct measurement of strain rate by experiment.

- ✓ Development of constitutive models
- ✓ Understanding the physical process involved in dynamic failures.

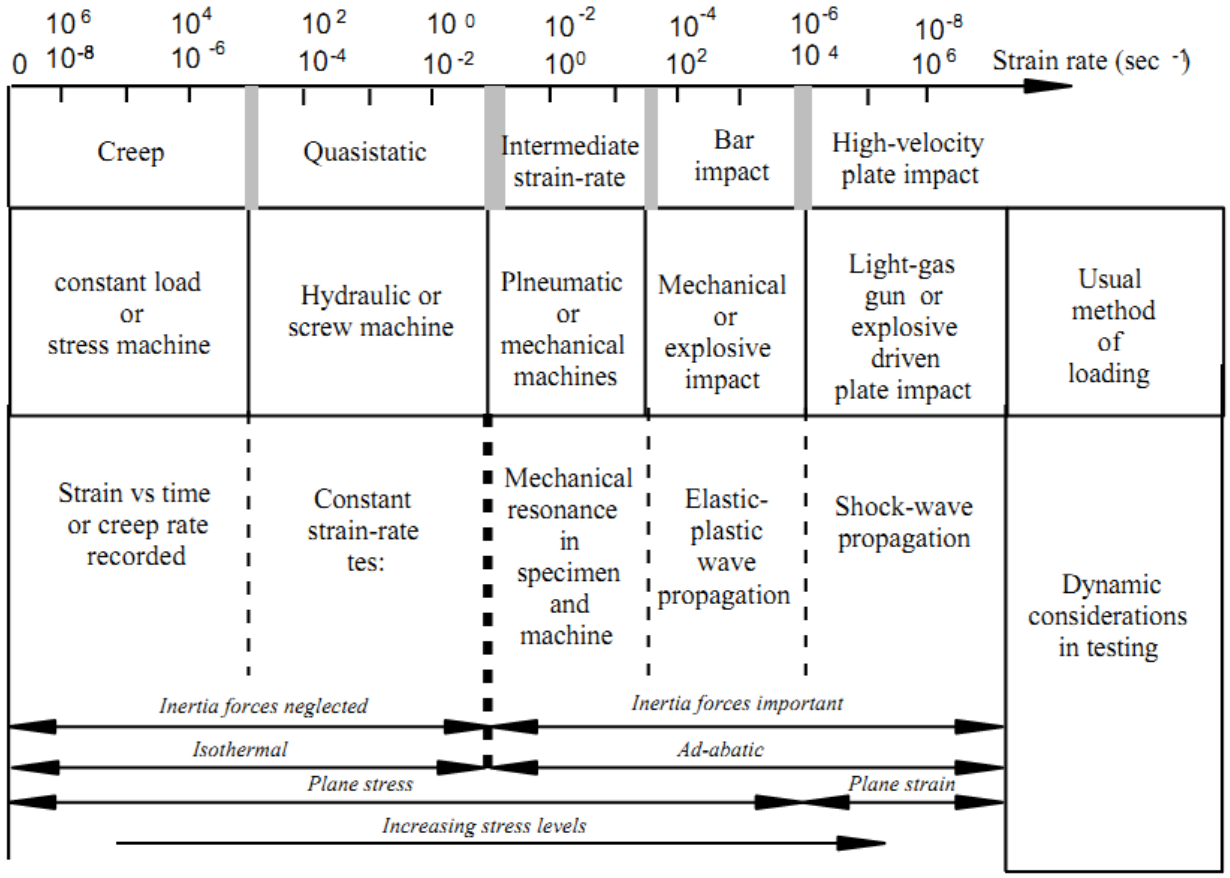

Figure 3 Dynamic aspects of mechanical testing

For the present paper the research concentrates on slow speed impact the strain range considered is Quasi- static which is for each tests the strain rate is a constant. Here hydraulic testing machine is used to test the specimen with the above mentioned strain rate rang for tensile load. [26] He also presented the stress-strain response of these steels were measured at seven strain rates between 0.003 s^{-1} and 1500 s^{-1} (0.003, 0.1, 30, 100, 500, 1000, and 1500 s^{-1}) and temperatures of 21, 150, and 300 °C. In addition, the steels were tested in both the unreformed sheet condition and the as-formed tube condition, so that tube forming effects could be identified. The strain rates below 10^{-6} s^{-1} 4occur in creep related applications and are tested using dead weights. The strain rates above 10^{-6} s^{-1} and below $5x10^{-1}$ s^{-1} are incurred in quasi-static loading of materials and are typically tested using a servo hydraulic testing machine [22]. He showed in the figure

below the strain rate ranges and different apparatus used as well as their corresponding application.

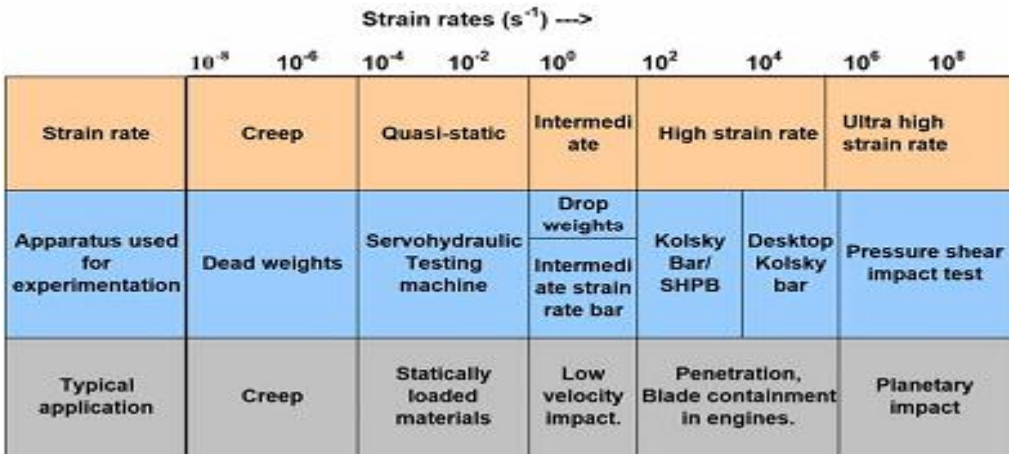

Figure 4 Experimental setups and applications for testing of materials.

2.3. Experimental Methods and Procedures

The size and geometry of the specimens as well as the testing procedure are in accordance with ASTM Standard E 8 (1981) for tension testing. Under this standard a nominal gauge length of 50 mm and a gauge of 12.5 mm are utilized in preparing the specimens. For mechanical tests, the specimens are mounted on a dynamic material testing system (MTS) and pulled to fracture at room temperature with a constant cross-head speed of 0.0083 mm s^{-1}, which corresponds to an initial strain rate of 3.3×10^{-4} s^{-1} (if all the crosshead movement is transmitted to the specimen), in order to obtain the room temperature flow properties. A strain-gage extensometer with a nominal gauge length of 25mm is utilized to measure the deformation of the specimens and the cross-head motion relative to the central pull-bar. The mechanical properties, such as ultimate tensile strength, yield strength, and percentage reduction area, are calculated from the stress – strain diagrams obtained from the tensile testing, in which the latter three specimens under identical conditions are used [27]**.**

[15], introduced the Standard tensile tests were generally conducted according to ASTM International (ASTM) E 8-01, "Standard Test Methods for Tension Testing of Metallic Materials" using a closed-loop, servo-hydraulic or a screw-driven, electro-mechanical test machine. In most cases, yield strength determination was made at a running crosshead rate that

produced post-yield strain rates between 0.001 min^{-1} and 0.005 min^{-1}. In some tests the extension rate was increased to produce a plastic strain rate of 0.05 min^{-1} for tensile strength determination. In other cases, the entire test was conducted at a constant extension rate. Several tests were conducted at a slightly higher extension rate 0.0325 mm/s, which produced plastic strain rates that conform to ASTM A 370-67, the test method used by steel mills to qualify steel. Much of the recovered steel was damaged in the collapse of the towers or subsequent handling during clearing of the WTC site. Specimens were selected from the least deformed regions. Even so, some of the resulting stress-strain curves of the low-strength steels do not exhibit a yield point. In such cases, yield strength was determined by the 0.2 percent offset method as specified in ASTM E 8-01. The geometrical and thickness differences in the various components did not allow for single, standard specimen geometry for the tensile testing. Specimen strain was measured using class B2 extensometers that conformed to ASTM E 83, "Standard Practice for Verification and Classification of Extensometer System." Total elongation was calculated by measuring gauge marks on the specimen prior to testing and again following fracture. Reductions of area for the round specimens were measured by comparing the original cross-sectional area to the area of the minimum cross section at the fracture location. Reductions of area for the rectangular and square cross section specimens were calculated based on the parabolic shape of the fracture surface, according to note 42 of ASTM E 8-01. The Figures show the various tensile specimen configurations used during this study. Although this study considered more than 10 types of specimen configuration but here for the purpose of relating the ideas with this paper the related specimen configuration is discussed here.

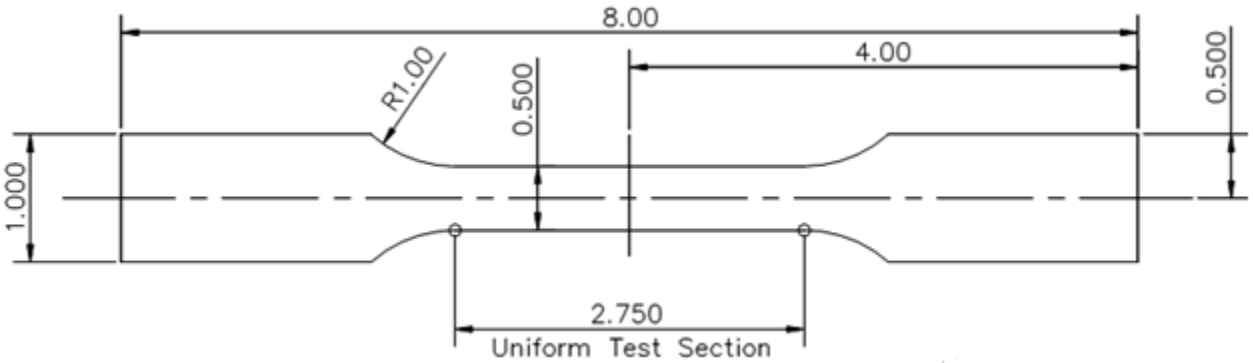

Figure 5 Flat tensile specimen typically used for standard room-temperature quasi-static tensile tests**.**

Another specimen configuration is prepared ready for tensile test is introduced by [22] Figure 6. shows the flat dog bone specimen designed for tension testing of Ti64. The gage section is 0.200” long, 0.080” wide and 0.027” thick. A radius of 0.050” is provided at the corners so as to make sure there are no stress concentration effects.

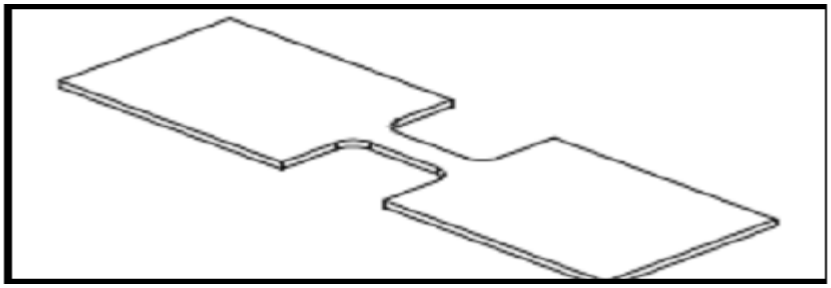

Figure 6 A flat dogbone Ti64 specimen for tension tests

And many dynamic test methods are available but according to their application and availability of them in Ethiopia and particularly in Addis Ababa University none of the following testing method except tensile testing using servo hydraulic universal testing machine are presented or applied for this paper but as a method they are cited here. And they are discussed by [24]according to his research each of these test methods can be used to describe a certain range of load/strain rates and each technique can be used to obtain particular information on the dynamic response and behavior of materials**.**

2.3.1. Dynamic Test Methods

- Punch Tests
- Izod, Charpy Impact
- Drop Weight Tests
- Hydraulic/Pneumatic Machines
- Hopkinson Pressure Bar
- compression
- tension
- shear
- flexure
- Flyer Plate

Some specific comments on each of the test techniques follow.

Punch Tests are related to loading rate and generally used on beam and plate type specimens. Information obtained from such tests is related to the maximum punch load for a given speed of load.

Charpy/Izod Tests are related to loading rate and generally used on beam specimens which may be notched or unnotched-notched. Such tests are often used as part of a standardized testing program for obtaining information on material energy absorption, notch sensitivity, and the type of failure/fracture occurring in the material.

Drop Weight Services are related to loading rate and are generally used on beam and plate type specimens. Data obtained relates to material energy absorption, fracture toughness, failure mechanisms, and notch sensitivity.

Hydraulic/Pneumatic Devices test material strain rate sensitivity in specimens loaded in a uniaxial test mode. Data obtained from such tests in addition to material rate sensitivity include mechanical properties and material failure modes.

Hopkinson Pressure Bar Tests are used in a tensile, compressive, torsion or flexure mode of loading. Data obtained for such tests include information on material strain rate sensitivity, stress plus shaping, constituent properties, dynamic ultimate stress, fracture mechanisms, constitutive equation modeling, pulse attenuation and damage initiation.

Plate Impact/Flyer Plate Experiments are performed at very high loading and strain rates. Data obtained from these tests include information on spell information, failure processes, material properties degradation, stress wave induced damage, and constitutive modeling parameters.

Of the test techniques cited, pressure bar tests represent one of the most widely used test techniques for investigating the strain rate sensitivity of metals and composite materials. In this present work servo-electrohydraulic testing machine is used to load each sample specimen in tension to get mechanical behavior of the material under study. This apparatus is used in this research because of its maximum capacity restriction: max.crosshead speed of 15mm/min and

600kN maximum load generated by the machine and so the strain rate is also forced to be restricted in the quasi-static ranges.

2.4. Bumper

In automobiles, a bumper is the front-most or rear-most part, ostensibly designed to allow the car to sustain an impact without damage to the vehicle's safety systems [17].

Figure 7 Show a BMW front bumper (highlighted in red) [17].

2.4.1. Purpose of a bumper system

Minimize damage or injury by absorption of energy through elastic and, eventually, plastic deformation during frontal and rear collisions with pedestrians, other vehicles and fixed obstacles at relatively low velocities.

Legislative and insurance test procedures are found in FMVSS 581, EC 78/2009 and RCAR member sites. They specify the conflicting requirements of a soft absorber for pedestrian safety with the following functionality:

- Prevent structural and visible damage resulting from low speed impacts
- Minimize cost of repair (insurance rating) resulting from medium speed (15 km/h) impacts
- Manage load path and structural integrity for higher speed impacts to maximize occupant protection.

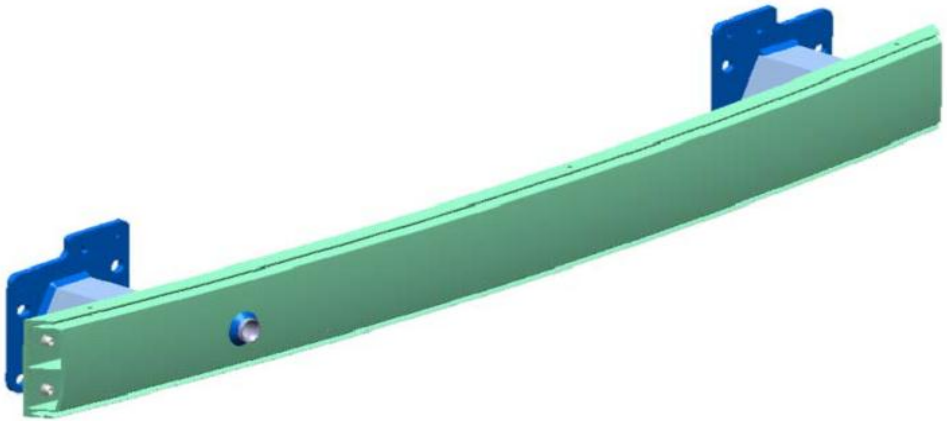

Shows the bumper beam with crash box (source: [4])

The overall objective remains to reduce the aggressiveness of the crash event. These issues are solved through controlled crash deformation. This case study deals with the effectiveness of the crash management system, composed of the bumper and the crash tubes [4].

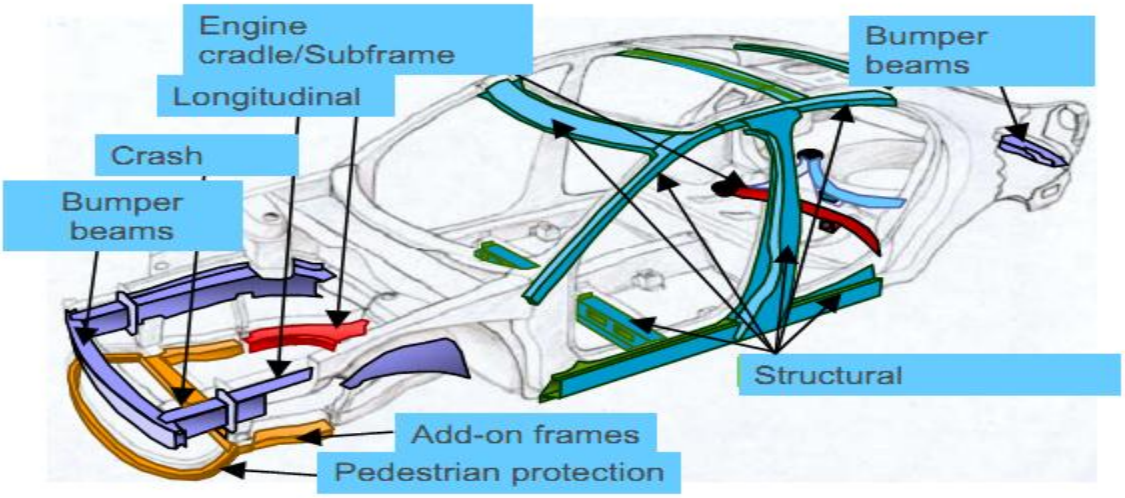

Composed of the bumper and the crash tubes (source: [4])

2.4.2. A Bumper System and Components

A bumper system consists of three components (as shown in Figure 8) such as plastic fasica, energy absorber and bumper beam. A brief description about components is furnished in the following sub-section.

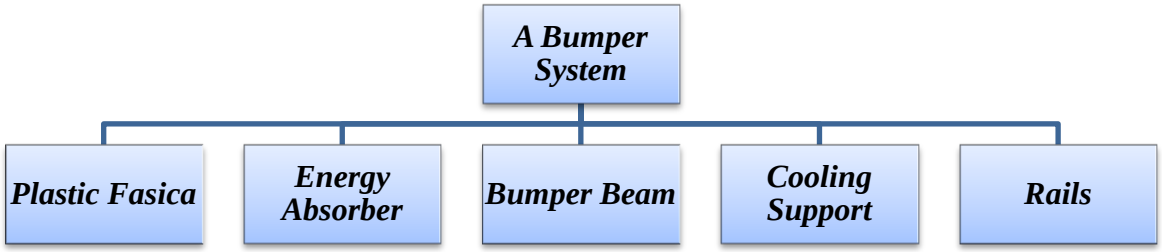

Figure 8 Shows the Automotive bumper system and components

2.4.2.1. Fasica

Bumper fasica is designed to meet several requirements. It must be aerodynamic to control of the air around the car and the amount of air entering the engine compartment. It should be aesthetically pleasing to the consumer. Typical fasica are styled with maney curve and ridges to give the bumpers dimension and distingush vehicles from competing models. Another requirement of bumper fasica is that theybe easy to manufacture and to fabricate. It is also important for it to light in weight. Virtually all fasicas are made from one to three materials: polypropylene, polyurethane .

Figure 9 Shows the fasica part of the bumper system [9]

2.4.2.2. Energy Absorber

Energy absorbers are designed to absorb a portion of the kinetic energy from a vehicle collision. Energy absorbers are very effective in low speed impact, where the bumper springs back to its original positions. In order to comply with U.S federal regulation, manufacturers fit their bumpers with energy absorbers. Generally energy absorbers are mounted between face bar/bumper reinforcement and the frame. There are three types of energy absorbers. The most common is similar to shock absorbers. The typical bumper shock is a cylinder filled with hydraulic fluid. Upon impact, a piston filled with inert gas is forced into cylinder. Under pressure, the hydrualic fluid flows into the piston through small opening. The controlled flow of fluid absorbs the energy of the impact. When the force of the impact is relieved, the pressure of the compresses gas forced the hydrualic fluid out of the piston and back into the cylinder. This action forces the bumper back to its original position.

Another type of energy absorber is found on many light motors and sport model vehicles. Instead of shock absorbers, foam is mounted between the fasica and the face bar or reinforcement bar, where a thick urethane foam pad is sandwiched between impact bar and a plastic face bar or cover. On some vehicles the impact bar is attached to the frame with energy-absorbing bolts. The bolts and brackets are designed to deform during collision in order to absorb some of the impact force. The bracket must be replaces in most collision repairs [16] Energy absorber types include foam, honeycomb and mechanical devices. All foam and honecomb absorbers are made from one of the three materials: polypropylene, polyurethane or low density polyurethane. Mechanical absorbers are metallic and resmble shock absorbers. In some bumper systems, the reinforcing beam itself is designed to absorb and separate energy absorbers are not required. Here in this paper the energy absorber is metallic recatngular shaped shell which resmble the shock absorber and made in the shape of s-beam which assembled to the bumper beam to assist in absorbing energy when the bumper is struck then it buckles by providing both energy absorbing and energy- storing effect. After the impact, the energy stored in in the s-beam rectangular shaped shell returns the unit and the bumper to its original posion.

The main purpose of an automotive bumper beam is to protect the passengers of vehicle from injuries in a low speed collision. The automotive bumper system also to protect the hood, trunk,

fuel, exhaust and cooling system as well as safety related equipment. The purpose of a bumper system is to minimize damage or injury by absorption of energy through elastic and, eventually, plastic deformation during frontal and rear collisions with pedestrians, other vehicles and fixed obstacles at relatively low velocities. The function of automotive bumper has changed considerably over the past 70 years. The later performance is achieved by a combination of careful design and materials selection to obtain a particular balance of stiffness and strength and energy absorption that is unique to each platform. Energy absorption is important criterion, because the bumper must limit the amount the impact force it transmits to the surrounding rails and vehicle frame. Automotive bumper plays a very important role not only in absorbing impact energy (original purpose of safty) but also in styling stand point. A great deal of attention with in the automotive industry has been focused upon light weight and sufficient safety in recent years. Therefore, the bumper system equipped with bumper beam and energy absorbing element is a new world in the market [6]. In this work the author selected composite materials for this car safety system considering weight with corresponding fuel consumption but in the present study the material under study is the low carbon steel considering its ductility with maximum energy absorption during slow speed collision. Not only the energy absorption but also the easiness of formability, recyclability of the material unlike the composite materials.

[3] Here the report considers several factors that an engineer must consider when selecting a bumper system. The most important factor is the ability of the bumper system to absorb enough energy to meet the OEM's internal bumper standard. Another important factor is the bumper's ability to absorb energy and stay intact at high-speed impacts. Weight, manufacturability and cost are also issues that engineers consider during the design phase. Both initial bumper cost and repair cost are important. The formability of materials is important for high-sweep bumper systems. Another factor considered is recyclability of materials, which is a definite advantage for steel. Both the last factor and the energy absorption factors are the main aim and agreement of the present research with the above stated report most importantly the current work considering steel samples from two industries in Ethiopia with different compositions and assumed to be taken from the bumper beam and tested using universal testing machine for different strain rate and in the quasi-static ranges. And their energy absorption during deformation under applied load is calculated from load versus elongation graph is calculated and the best material is selected for the bumper beam. Figure 9 from A-D below shows the different bumper system.

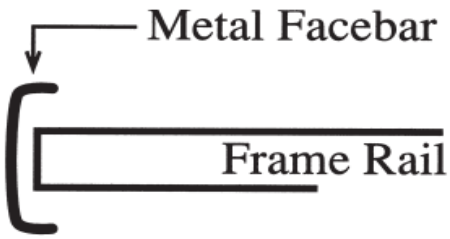

(A).

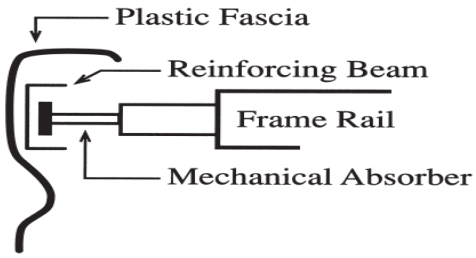

(C).

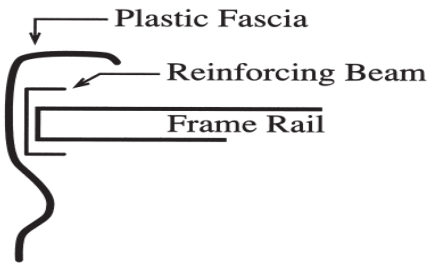

(B).

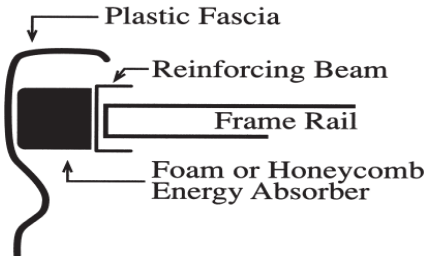

(D).

Figure 10 Four different types of automotive bumper systems: A) Metal face bar system, B) plastic fasica and reinforcing beam system, C) plastic fasica, reinforcing beam and energy absorbers and D) plastic fasica, reinforcing beam and foam or honeycomb energy absorbers

2.4.2.3. Bumper Beam

The reinforcing bumper beam is the key component of the bumper system that helps to absorb the kinetic energy from a collision and provide protection to rest of the vehicles. By staying intact during a collision, the preserves the frame. Design issue for the reinforcing beam includes strength, manufacturability, weight, recyclability and cost. Current bumper system employs steel to produce the bumper beam. Steel reinforcing beam are depth of draw (stamping), Sweep (roll formed) or made by the Planja process (hot stamping process).

A stamped beam is advantageous in high-volume production and offer complex shapes. However, the stamping process is capital intensive and this process itself requires good formability from the steel. The planja process in a hot stamping process, which results in high-strength beam and is relatively expensive due to its low production rate. The sheet metals are continuously fed into a gas fired furnace and heated to austenitizing temperature, approximately 900 ^{0}C, in about 3 to 5 minutes. Then the material is fed into hydraulic press. The press cycles down, remaining in that position while the dies quickly cool the formed steel until the temperature is approximately 40 ^{0}C, well below the martensitic finish temperature. The required to cool the parts in the dies is 10 seconds per mm of thickness. Roll foam beam accounts for the majority of the steel reinforcing beam used today. Common cross section for roll foam beams are box, C or channel, and hat shapes. All steel reinforcing beams are better corrosion resistant. Some beams are made from hot dip galvanized sheet. The zinc coating on these products provides excellent corrosion resistance properties [5]. The Figure 10 A & B below shows the different types of process to have the bumper beam.

The definition of depth of draw and sweep which is stated by American Iron and Steel Institute is as follows:

Sweep expresses the degree of curvature of the outer bumper face, or the face farthest removed from the inside of the vehicle. Sweep is defined in Figure 10 shown below [2].

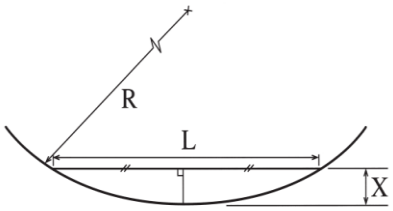

(a)

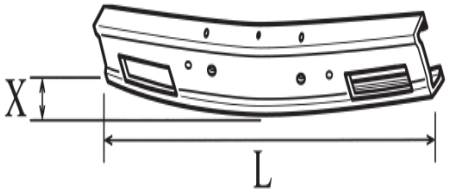

(b)

Figure 11(a) and (b) Shows definition of sweep

Depth of draw is often used to describe the amount of rounding and wrap around on a bumper section, and in particular, a stamped face bar. As shown in Figure 5.2, depth of draw is the distance, X, between the extreme forward point on a bumper and the extreme aft point on a

bumper. This distance has a physical significance in that it cannot exceed the opening available with a given stamping press. X is usually stated in inches (millimeters) [2].

Figure 12 a) toyota camryno. 35 sweep source: [2]

Figure 13 Definition of depth of draw [2]

Figure 14 b) ford f150 pickup 559mm (22 inches) depth of draw with 50xlf steel. Aerodynamic styling source: [2]

2.5. Energy Absorption

The modern system has the function of absorbing the energy of low speed crash, thus avoiding higher vehicle damage. The energy Absorption (EA) capability of the bumper system is during a low speed crash is evaluated by the load – displacement response. The area under the load-stroke diagram is a measure of the energy absorbed. During low speed impact, the bumper system has the function of preventing damage to the body-in-white (BIW). Hence the maximum displacement impact load transmitted through the system has to be limited. The maximal displacement is specified by the vehicle design [18]. And presented here as follows

$$EA = \int F dl \qquad \text{(Equation 3)}$$

The energy absorption is calculated using total energy during the impact for every displacement interval. The absorption energy, E *absorbed*, is expressed as equation below

$$Easorbed = Total\ energy - Kinetic\ energy \quad (Equation\ 4)$$

2.5.1. The Specific Energy Absorption (SEA)

As expected, the energy absorption becomes higher as the thicknesses increase. However, in order to compare between thicknesses, the Specific Energy Absorption (SEA) is calculated by dividing the energy absorb by the bumper beam mass as in equation below:

$$SEA = \frac{E_{absorb}}{m_{beam}} \quad (Equation\ 5)$$

As the result, 2.0 mm thickness shows amazing performance and the different of SEA between other thicknesses is low. As for the deflection, it decreases as the thicknesses increased [11].

3. Methodology

3.1. Experimental Method

3.1.1. Introduction

Mechanical testing plays an important role in evaluating fundamental properties of engineering materials as well as in developing new materials and in controlling the quality of materials for use in design and construction. If a material is to be used as part of an engineering structure that will be subjected to a load, it is important to know that the material is strong enough and rigid enough to withstand the loads that it will experience in service. As a result engineers have developed a number of experimental techniques for mechanical testing of engineering materials subjected to tension, compression, bending or torsion loading.

3.1.2. Description of the Experiment

This experiment is done to get the property of the sample materials which are three in number and they all are low carbon steel that is because it contains approximately 0.05–0.15% carbon. The tension test is done at Addis Ababa institute of Technology department of mechanical engineering in Mechanical workshop. The sample material from the bulk material of the bumper is taken to be tested in our laboratory for tensile strength. The samples are prepared according to ASTM E8 standards in order to achieve the experimental objective. The tensile testing is done using the servo electrohydraulic universal testing machine with data acquisition in order to have the X-Y data information during the testing of the specimen. The experiment is done by applying load from the servo hydraulic universal testing machine by applying tension uniaxial load on one side of the specimen and the other side is constrained to be fixed. The measurement is taken on the gauge section in which its length is 50mm, 2mm thick and 12.5mm width. Tensile testing resembles cold working or strain hardening because the process or the experiment is done

without temperature or most of the time it is done at room temperature and below recrystallization temperature. The required outputs from the data acquisition on the stress-strain curve are: 0.2% yield strength, ultimate strength, young's modulus, ductility (percentage elongation and percentage reduction in area) and the final elongation at fracture is measured.

3.1.3. Theoretical Background

The parameters under tensile experiment are very important to deal with most impact problems such as car impacted by another car during slow speed collision moment the material is strained (deformed) there by absorbing energy depending on the material type and mechanical properties which is the main concern of this paper. The specimen under study for this paper is assumed to be taken from the bulk material in question i.e. the Bumper beam. Here in this theoretical part of the experiment principles and some equation related to the experiment are presented and later on used to analyze the results.

Mechanical properties that are important to a design engineer differ from those that are of interest to the manufacturing engineer.

- **In design**, mechanical properties such as elastic modulus and yield strength are important in order to resist permanent deformation under applied stresses. Thus, the focus is on both elastic and plastic properties. The yield behavior of a material is determined from the stress-strain relationship under an applied state of stress (tensile, compressive or shear).This lab introduces the uniaxial tensile test to determine the basic mechanical properties of a material.

3.1.4. Basic Principles

The following principles are followed during the tensile testing of the specimen

- An axial force applied to a specimen of original length (lo) elongates it, resulting in a reduction in the cross-sectional area from Ao to A until fracture occurs. The load and change in length between two fixed points (gauge length) is recorded and used to determine the stress-strain relationship.

Some of the futures take place on the specimen during testing

In the diagram (right)

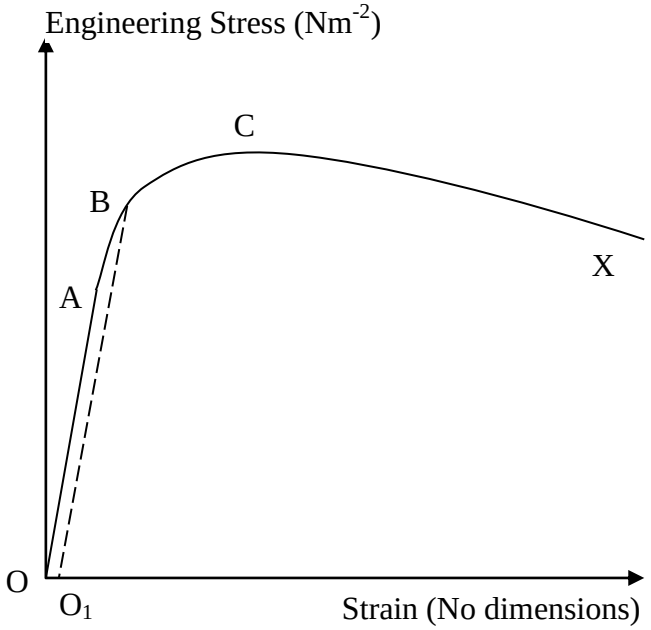

Figure 15 different regions of stress vs. strain graph

O = Initial origin

OO_1 = Permanent elongation

A = Elastic limit

OA = Linear region

B = General point beyond A

BO = Relaxation if stress removed

(Note: O_1B is parallel to OA)

C = Maximum Strength

AC = Region of plastic Deformation

X = Failure

CA = Plastic Flow

(Note: This is the region where "necking" or localised thinning of the specimen takes place.)

Primary Test Output:

The primary output from a tensile test is the load vs. elongation curve of the specimen, which is recorded in real-time using a load cell and an extensometer. This curve is then used to determine two types of stress-strain curves:

- Engineering stress-strain
- True stress-strain

Engineering Stress and Strain:

- ✓ These quantities are defined relative to the original area and length of the specimen. The engineering stress (σe) at any point is defined as the ratio of the instantaneous load or force (F) and the original area (Ao).The engineering strain (e) is defined as the ratio of the change in length (L-Lo) and the original length (Lo).

$$\sigma_e = \frac{F}{A_O} \qquad (Equation\ 6)$$

$$e = \frac{L - L_O}{L_O} \qquad (Equation\ 7)$$

- ✓ The engineering stress-strain curve (σ_e- e) is obtained from the load-elongation curve. The yield point, called the yield strength (Y), signifies the start of the plastic region. It is very difficult to find the actual yield strength experimentally. Instead, we use a 0.2% offset yield strength. 0.2% offset yield strength is the point on the curve which is offset by a strain of 0.2% (0.002) [the intersection of the curve with a line parallel to the linear elastic line and is offset by a strain of 0.002] The stress at maximum (Fmax/Ao) is referred to as the Ultimate Tensile Strength (TS) and signifies:
  - The end of uniform elongation.
  - The start of localized necking i.e. plastic instability.

True Stress and Strain:

- The true stress (σ) uses the instantaneous or actual area of the specimen at any given point, as opposed to the original area used in the engineering values

$$\sigma = \frac{F}{A} \qquad (Equation\ 8)$$

The true strain (ε) is defined as the instantaneous elongation per unit length of the specimen

$$\varepsilon = \int_{L_O}^{L} \frac{dL}{L_O} = \ln \frac{L}{L_O}$$ (*Equation 9*)

The relationship between the true and engineering values is given by:

$$\sigma = \sigma_e(1 + e\ )$$ (*Equation 10)*

$$\varepsilon = \ln(1\ + e)$$ (*Equation 11*)

From the experiment for a given value of the load and elongation, the true stress is higher than the Eng. Stress, while the true strain is smaller than the Eng. Strain

Ductility is the degree of plastic deformation that a material can withstand before fracture. A material that experiences very little or no plastic deformation upon fracture is termed brittle.

In general, measurements of ductility are of interest in three ways:

1. To indicate the extent to which a metal can be deformed without fracture in metal working operations such as rolling and extrusion.

2. To indicate to the designer, in a general way, the ability of the metal to flow plastically before fracture.

3. To serve as an indicator of changes in impurity level or processing conditions. Ductility measurements may be specified to assess material quality even though no direct relationship exists between the ductility measurement and performance in service.

Ductility can be expressed either in terms of percent elongation (z) or percent reduction in area (q);

$$z = \%\Delta l = \left[\frac{(lf - lo)}{lo}\right] \times 100$$ *(Equation 12)*

$$q = \%RA = \left[\frac{(Ao - Af)}{Ao}\right] \times 100 \qquad \textit{(Equation 13)}$$

Resilience is the capacity of a material to absorb energy when it is deformed elastically.

Toughness is a measure of energy required to cause fracture.

Poisson's Ratio is the lateral contraction per unit breadth divided by the longitudinal extension per unit length.

Strain Hardening:

- ✓ In the plastic region, the true stress increases continuously. This implies that the metal is becoming stronger as the strain increases. Hence, the name "Strain Hardening". The relationship between true stress and true strain i.e. the flow curve can be expressed using the power law:

$$\sigma = K\varepsilon^n \qquad \textit{(Equation 14)}$$

Where **K** is called the strength coefficient and **n** the strain hardening exponent

The plastic portion of the true stress-strain curve (or flow stress curve) plotted on a log-log scale gives the n value as the slope and the K value as the value of true stress at true strain of one.

$$\log\sigma = \log K + n \times \log\varepsilon \qquad \textit{(Equation 15)}$$

For materials following the power law, the true strain at the UTS is equal to n.

In plotting the log-log plot, data points after the yield point (to avoid elastic points) and before instability (necking) are used. A material that does not show any strain-hardening (n=0) is designated as perfectly plastic. Such a material would show a constant flow stress irrespective of strain. K can be found from the y-intercept or by substituting n and a data point (from the plastic region) in the power law.

3.1.5. Experimental Design and Procedure

For this experiment first let us state experimental design then it follows the procedure followed.

3.1.5.1. Composition Identification

The composition for each materials is found by using spectrometer which found in our workshop since it doesn't work properly the spark test using grinder at velocity of 25 m/s is used to predict the rough estimation of the alloy and the carbon in the three sample material is estimated as follows using the criteria in the table below and in the figure

Table 2* shows the three specimen composition from spark test [**28], [29].**

Criteria's	*High Alloy Steel(HAS) M-2*	*Low Carbon Steel (LCS) M-3*	*Mild Steel (MS) M-1*
Volume of stream	*small*	*large*	*large*
Relative length	*0.6m*	*1.6m*	*1.4m*
Color at wheel	*red*	*white*	*straw*
Color at end	*red*	*white*	

M-1= material 1, M-2= material 2, M-3= material 3

M-1 M-2 M-3

Figure 16* shows the sparks of all the specimen while testing

3.1.5.2. Experimental Design

3.1.5.2.1. Factors, Levels and Replica

This are one of experimental parts that are going to be studied and most importantly it affects the response variables during experimental testing of the selected samples. So in this paper strain rate and the material type are considered. Strain rate and material type A, B and C as shown in the table1 below. So the factors become 2 and the levels are as shown in the

table 1. And the number of observation with considering the replica is equal to 3*12 =36 and it also indicates that number of experiment is performed

Table 3 The matrix of Experiment to be conducted under room temperature

Strain rate(s^{-1})	***3.33×10^{-3}***	***3.33×10^{-2}***	***3.33×10^{-1}***	***0.33×10^{1}***
Crosshead(mm/min)	***10***	***100***	***1000***	***10000***
MS	**X X X**	**X X X**	**X X X**	**X X X**
HAS	**X X X**	**X X X**	**X X X**	**X X X**
LCS	**X X X**	**X X X**	**X X X**	**X X X**

MS = Mild Steel , HAS = High Alloy Steel, LCS = Low Carbon Steel

3.1.5.1.2. Output Variables from the factors

The output or the dependent variables which are affected by the change of the independent variables or the factors for this tensile testing are decided by the statement of the problem and according to the intended application of this selected material from the above three types. And they are mentioned as follows:

- 0.2% yield stress
- Toughness (Energy or Area under the σ-ε curve)
- Percentage elongation (measure of ductility)
- Reduction in area (measure of ductility)
- Stress vs. strain curve

3.1.5.3. Procedures

For this particular research the equipment used for testing low carbon sheet metal loaded in tensile is the computer-electrohydraulic universal testing machine model series WAW-600, precision grade 0.5, serious no 16259 and datum 08.11 with maximum generated load of 600kN and maximum cross head speed of 10000mm/min and made in china. The testing machine is indicated in the figure below and according the type of loading there are two types of tensile testing machine they are

Screw Driven Testing Machine: During the experiment, elongation rate is kept constant.

Hydraulic Testing Machine: Keeps the loading rate constant. The loading rate can be set depending on the desired time to fracture.

From the two types the one employed for this current experiment is the hydraulic testing machine which is available in our workshop here in Addis Ababa University institute of Technology (AAiT).

3.1.5.2.1. Materials used

The materials under the test are three types in quantity and all are low carbon steel materials. These materials are shown below in the figure indicated by alphabet A, B and C.

Figure 17 shows the specimens "dog bone" used for tensile testing

Before the test

1. Put gage marks on the specimen
2. Measure the initial gage length and width since the specimen is plate
3. Select a load scale to deform and fracture the specimen. Note that tensile strength of the material type used has to be known approximately.

During the test

1. Record the maximum load
2. Conduct the test until fracture.

After the test

1. Measure the final gage length and Width. The width and thickness should be measured from the neck.

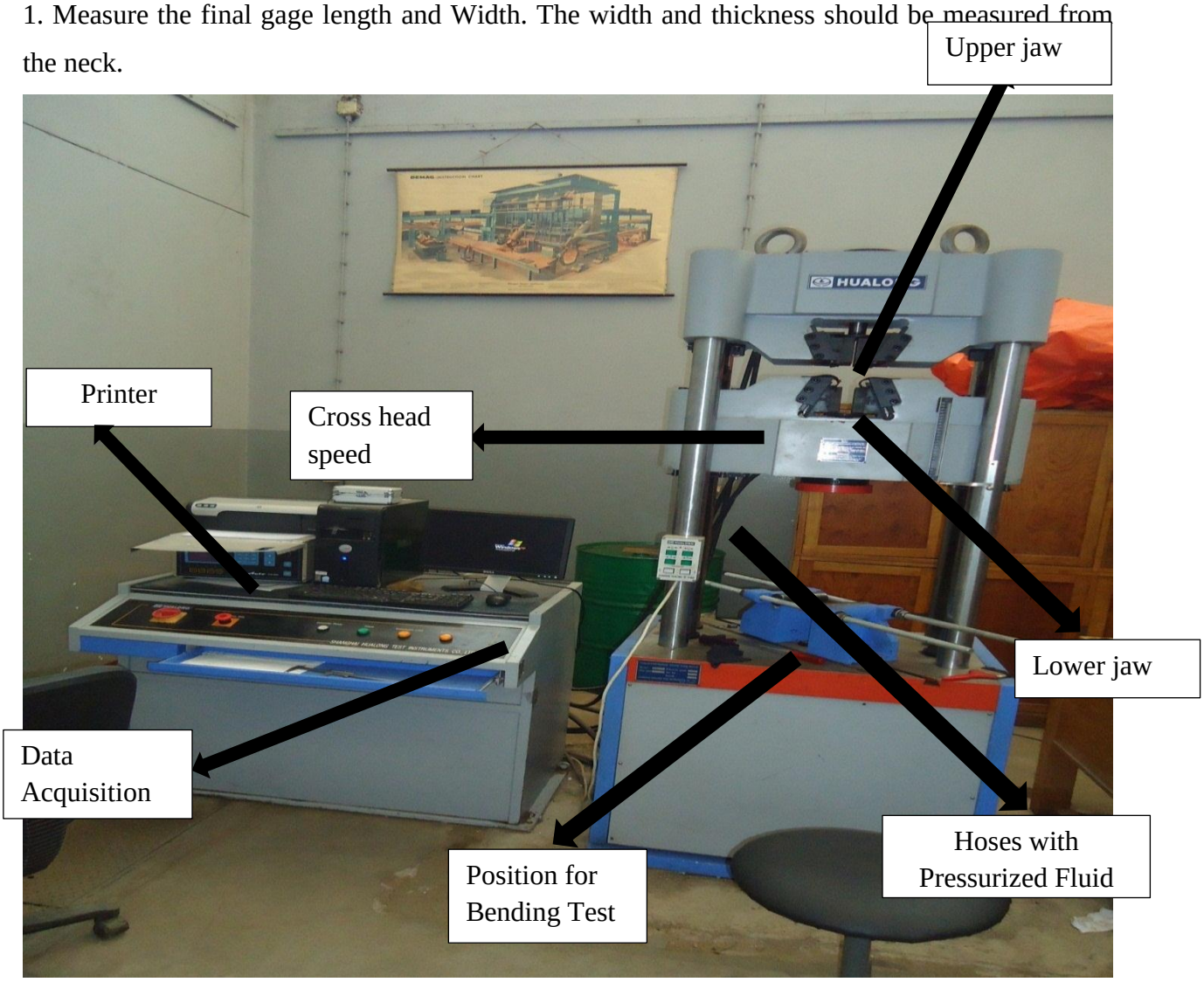

Figure 18 show the computer-electrohydraulic universal testing machine model: WAW-600

3.2. Finite Element Modeling

3.3.1. Breif introduction to ABAQUS/CAE Model

The simulation work was carried out using commercial software called ABAQUS/CAE which is an engineering tools for programming that is used to solve various degrees of engineering problems ranging from linear to non-linear problems that are complex. The sofware is used all over the globe in industries and also by academicians.

Abaqus is a suite of powerful engineering simulation programs, based on the finite element method, that can solve problems ranging from relatively simple linear analyses to the most

challenging nonlinear simulations. Abaqus contains an extensive library of elements that can model virtually any geometry. It has an equally extensive list of material models that can sim ulate the behavior of most typical engineering materials including metals, rubber, polymers, com posites, reinforced concrete, crushable and resilient foams, and geotechnical materials such as soils and rock. Designed as a general-purpose simulation tool, Abaqus can be used to study more than just structural (stress/ displacement) problems. It can simulate problems in such diverse areas as heat transfer, mass diffusion, thermal management of electrical components (coupled thermal-electrical analyses), acoustics, soil mechanics (coupled pore fluid-stress analyses), and piezoelectric analysis.

ABAQUS/CAE enables models to be solved as quickly as possible by simpley impoting the geometry under investigation with the right physical and material properties associated to it, meshing it, loading and also by applying the boundary conditions to the material to be modeled [24].

The reference bumper subsystem model was taken from one of the complete FEM car models Available in the NHTSA web site and imported into ABAQUS environment. The bumper subsystem was isolated from the complete car model and the remaining car body mass was substituted by an equivalent lumped mass at the center of gravity of the car, as shown in Figure 2. In ABAQUS, there are two approaches to analyze impact problems: standard and explicit methods. Because of the nature of crash problems which involve very large and critical modeling issues such as three dimensional contact problems, the non-linear Dynamic-Explicit solver was considered. Different material models were applied based on the material characteristics. For steel, materials data were taken directly from the original available model and imported after the conversion to yield stress plastic strain relation since ABAQUS asks for material test data in this format [13].

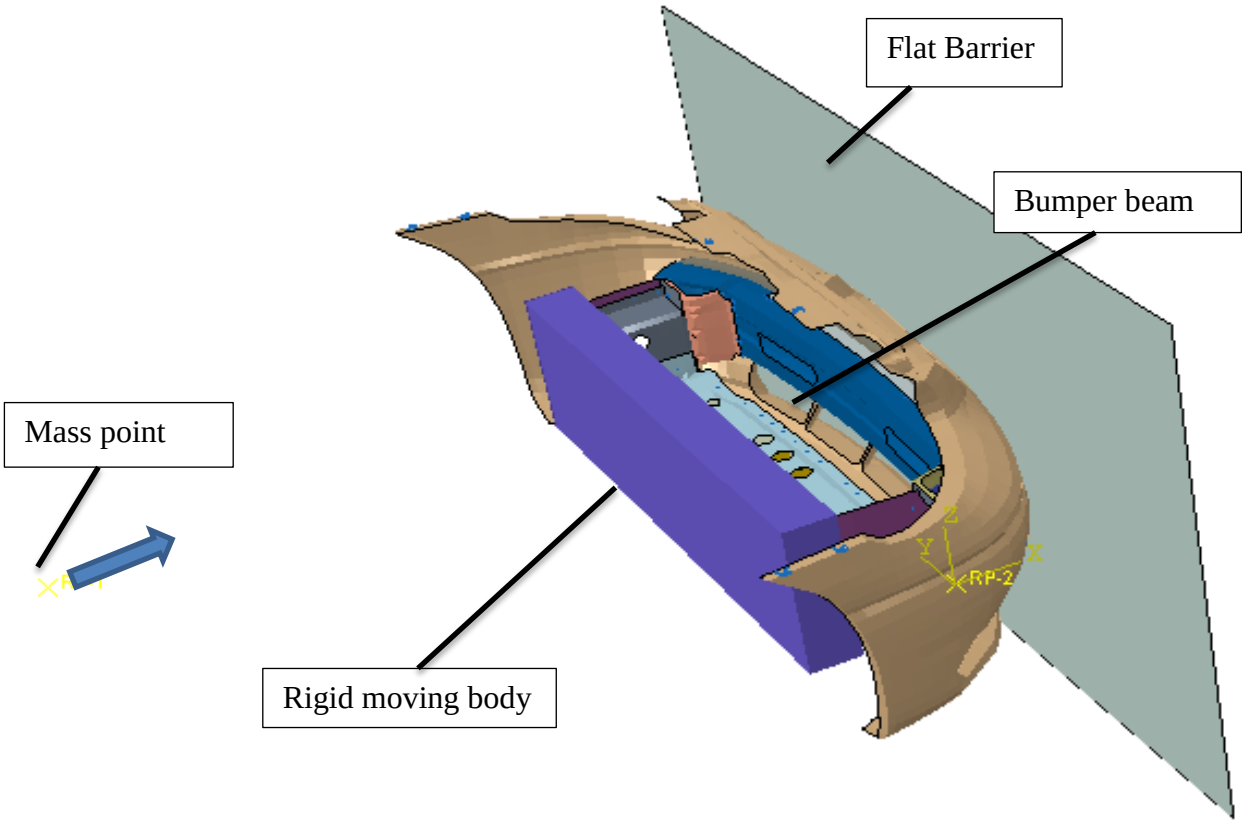

Figure 19 the isolated bumper subsystem from the complete car model and equivalent lumped mass

3.3.2. Algorithm of FEM Analysis

The flow of the work after analyzing experimental datas is shown below as follows

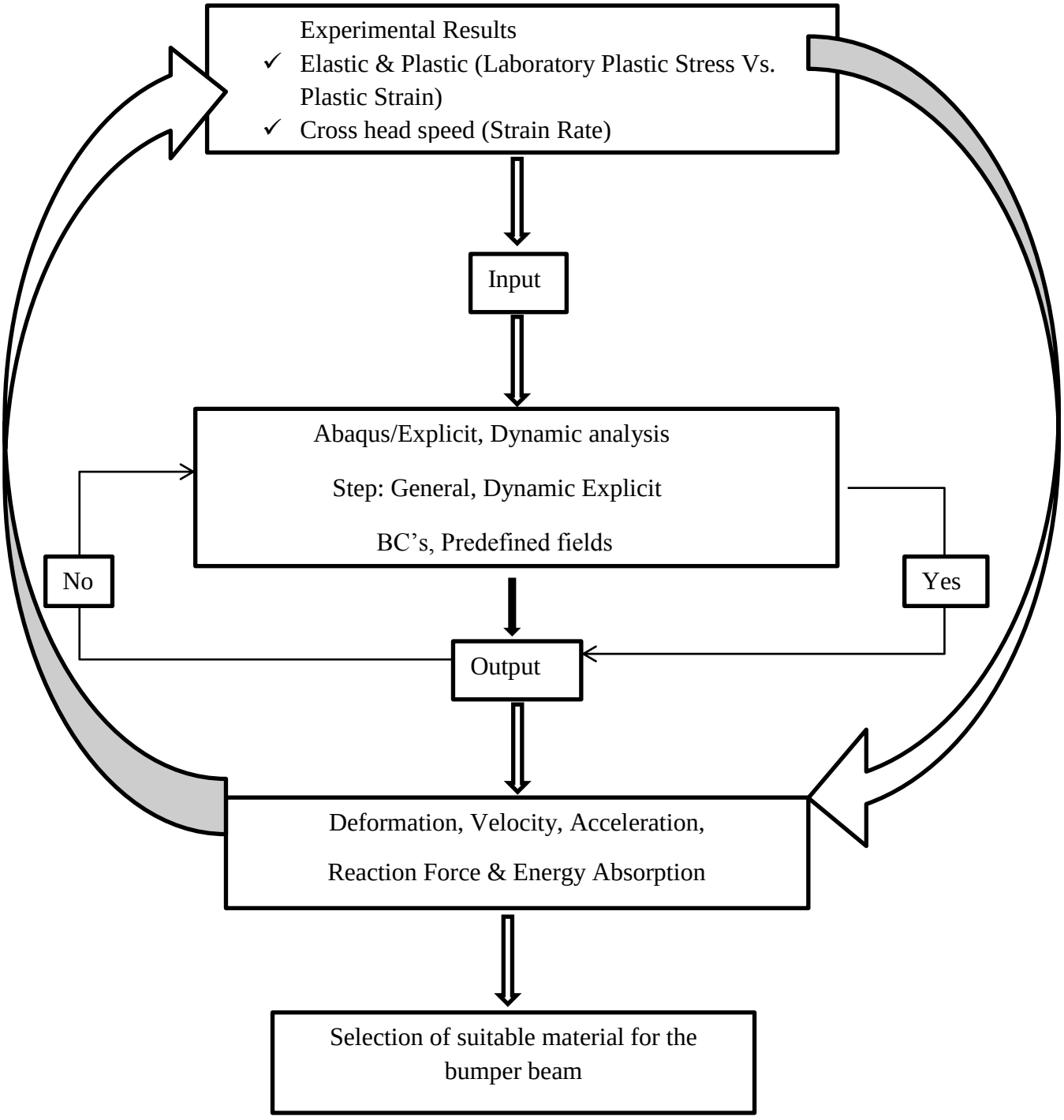

Figure 20 shows the algorithm of the ABAQUS/CAE model

3.3.3. The Processes for impact Analysis using ABAQUS/CAE

Pre-processing and post-processing and as it is briefly stated above it is put in the figure shown below. For this research the following steps are followed for the two process

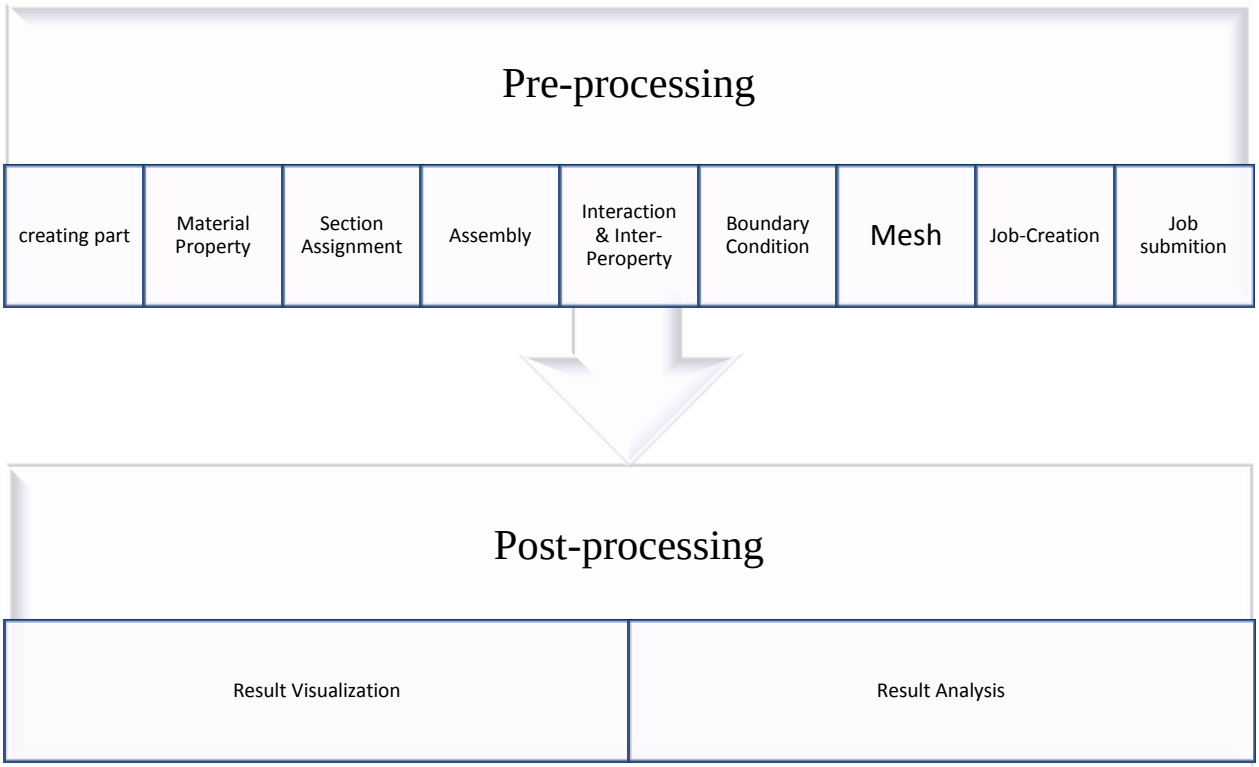

Figure 21 shows the two importnant process followed for the analysis of the slow speed impact

3.3.4. Input and Output of the problem using ABAQUS/Explicit

The algorithm of the Finite Element Analysis (FEA) software ABAQUS/CAE follow the following two processes: the first is during material property assignment where as the second is the final results during visualization which is the main objectives of the FEA.

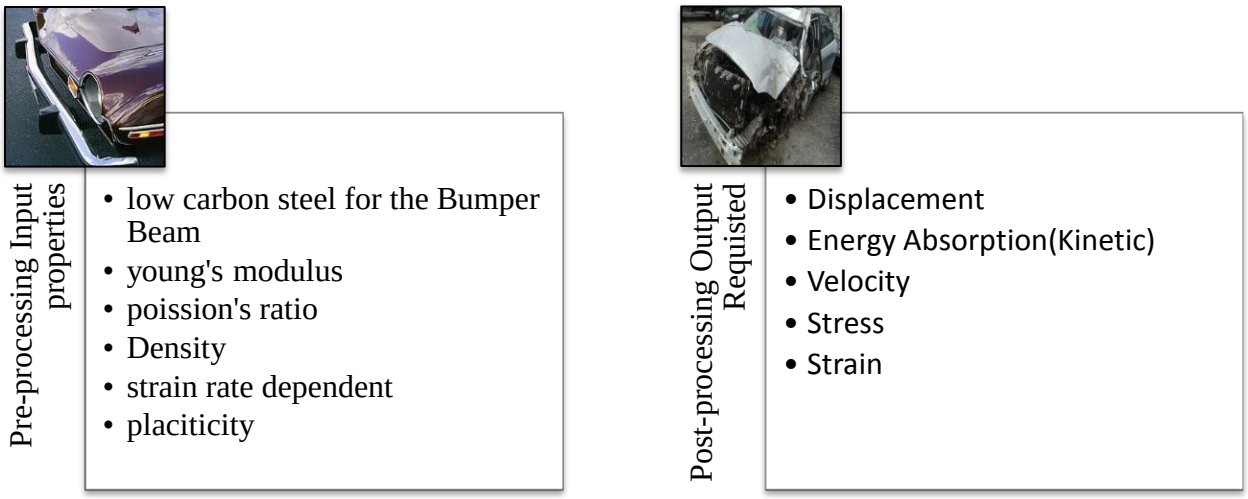

Figure 22 shows the algorithm followed for the FEA to get the desired solution to the problem

Pre-processing

In the pre-processing, the specimen was modeled and the input file stored which is illustrated by the following steps below.

Creating the part

The parts for this research are the car vehicle bumper beam parts which are created on Catia software and manufactured by one of the method of bumper beam manufacturing stated in the litrature review. They are rectangular and shell to consider the thickness and are shown in the figure below.

Figure 23 shows the Bumper Beam part 3D part work

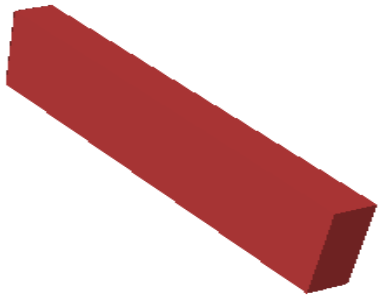

Figure 24 shows the rigid body which represents the car whole weight

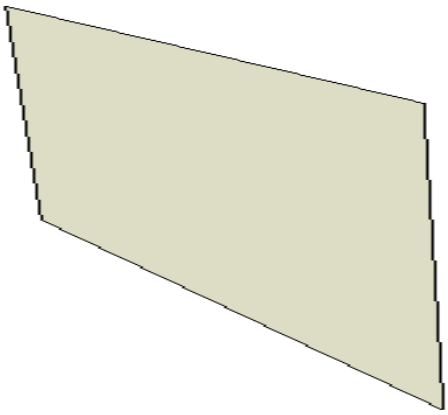

Figure 25 shows the rigid barrier which replaces another vehicle or rigid wall

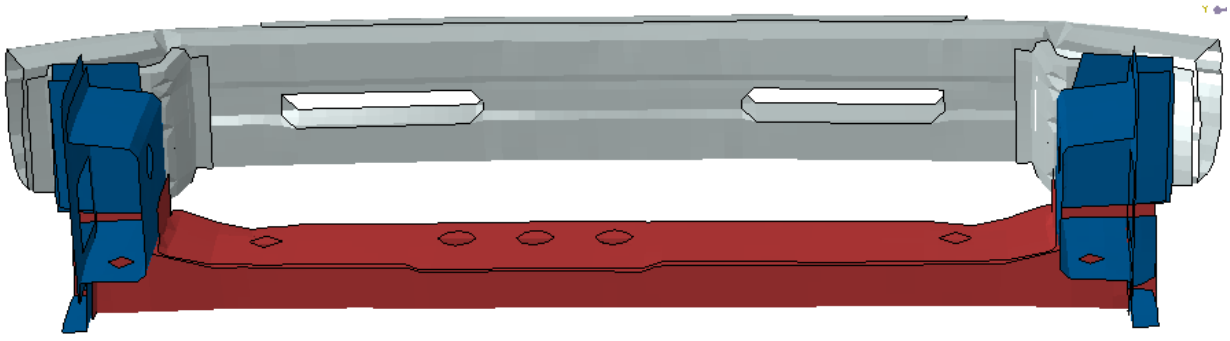

Figure 26 shows the bumper beam, cooling system support, and rails

Property Selection

This involves by defining and assigning material and section properties to the part, each region of the deformable body must refer to a section property which must include the material definition. In defining the section, the young modulus, poisso's ratio and yield stress were assigned to the part.

For this research the properties are added from the specimen responses after the test is done. The following properties in the table are used as input to the ABAQUS/CAE.

This material and property module part includes the following important feature:

- ✓ General
- ✓ Mechanical and
- ✓ Others

The properties like elasticity, placticity ,rate dependent and several material models are included under the mechanical option. Most inportantly this paper will major concern is the mechanical property used as input and and during visualizing in the viewport see the result to analyze the effect.

Defining linear elastic material behavior

The total stress is defined from the total elastic strain as:

$$\sigma = D^{el}\varepsilon^{el} \qquad \text{Equation 16}$$

where $\boldsymbol{\sigma}$ is the total stress ("true," or Cauchy stress in finite-strain problems), $\mathbf{D^{el}}$ is the fourth-order elasticity tensor, and $\boldsymbol{\varepsilon^{el}}$ is the total elastic strain (log strain in finite-strain problems). Do not use the linear elastic material definition when the elastic strains may become large; use a hyperelastic model instead. Even in finite-strain problems the elastic strains should still be small (less than 5%).

Directional dependence of linear elasticity

Depending on the number of symmetry planes for the elastic properties, a material can be classified as either isotropic (an infinite number of symmetry planes passing through every point)

or anisotropic (no symmetry planes). Some materials have a restricted number of symmetry planes passing through every point; for example, orthotropic materials have two orthogonal symmetry planes for the elastic properties. The number of independent components of the elasticity tensor $\mathbf{D}^{\mathbf{el}}$ depends on such symmetry properties. The simplest form of linear elasticity is the isotropic case, and the stress-strain relationship is given in Appendix F.

The elastic properties are completely defined by giving the Young's modulus, **E**, and the Poisson's ratio, **ν**. The shear modulus, **G**, can be expressed in terms of **E** and **ν** as $G = E/[2(1+\boldsymbol{\nu})]$ .These parameters can be given as functions of temperature and of other predefined fields, if necessary.

Creating an Assembly

Assembly contains all the geometry included in the finite element model. The assembly is initially empty, even though you have already created a part module. So you have to creat an instance of the part in the assembly module to include the model. The final assembled bumper beam system which is in its initial position is as shown in the figure below.

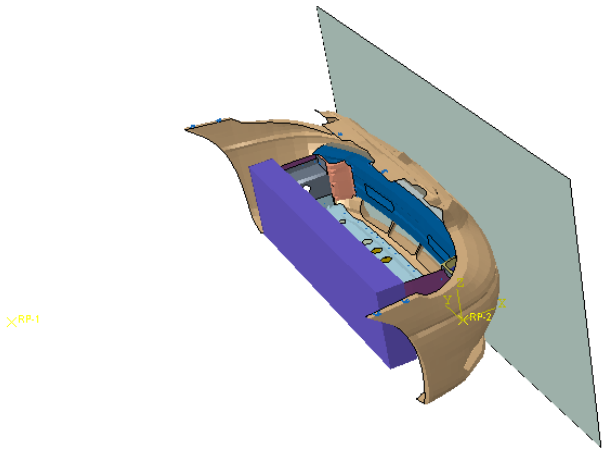

Figure 27 show the Assembly of the parts and in its initial postion

Step

In the step module, analysis step and output requist were defined, since interaction, load and boundary condtion can be step dependant. So the analysis step has to be defined before these can be specified. For the simulation General and Dynamic.explicit are defined.

Interaction

Interaction module is very important part of the finite element analysis when two or more objects are in contact. For this study the bumper beam with the rigid wall are modeld and the interaction properties are defined as for the tangential behavior frictionless hard contact and for the normal behavior rough hard (separable) contact. The former one is defined for the ineraction of the rigid body and the bumper beam with the crush box and rails. And later is defined for the interaction of bumper Subsystem and the rigid Barrier; which represents perhaps another vehicle or simply wall for this study. The contact property is show in the figure below:

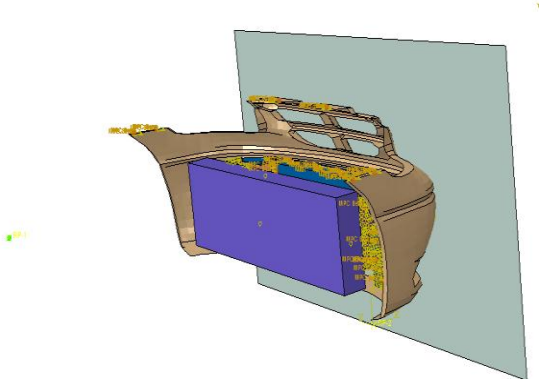

Figure 28 shows defining interaction property and contact property

Boundary Condition and Load

For this model, since there are two steps we apply BC's for each steps: the Accelerated and the Crush step. Here the impact plane is fixed using Encater initially and the bumper beam system has give a velocitiy for both steps for the accelerated and crush but inactive in the case of crush step this is done to creat room for movement. The velocity is in the direction of the impact and it is as shown in the figure below. Since this study involves experimental tensile testing in which the result is used as input to this FEA so predefined out field is requsted in the BC module or the load module. Among this predefined fields that of the temprature becouse at least the experimental test is performed at room temprature 300^{o}c is given as initial temp.

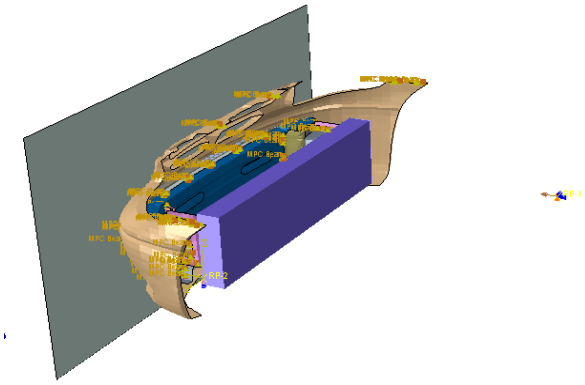

Figure 29 shows the Initial velocitiy of 1.11m/s in the direction of impact

Mesh

This is the module used to creat the finite element mesh where element library explicit and family shell and geometric order of linear as well as Quad reduced integration is used and S4R element type is used for the the whole bumper system and Quad is its element shape. Here the rigid barrier or the wall is defined analytical so its seed during meshing large.

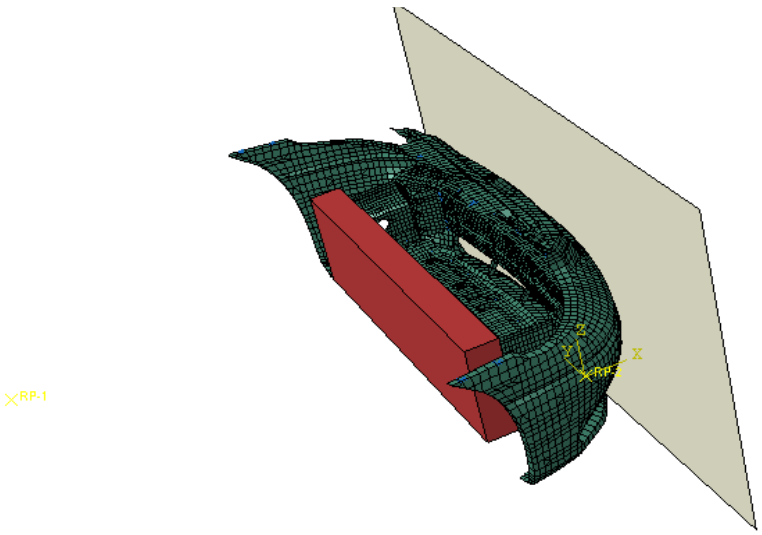

Figure 30 Shows the assembly mesh

Simulation

The final step of pre-processing, and it is done by creating a job. When all the parameters that are involved in the model are accomplished in the job module we select submit, to submit the job for analysis. While it is running we can moniter the analysis by obesrevining the different messages in the monitor windows like error, number of frame and most importantly warning to kill them.

Post-Processing

In the post-processing, the visualization module is used to view the results of the stress and strain distribution.

4. Result and Discussion

4.1. Experimental Results

In the figure30 below it is observed that the true stress will increases with the increase in strain rate for the same material for this paper the low carbon steel which is the 3rd material under investigation. And also the percentage increase in the maximum true stress will be almost 12.5% for the first two speed and almost the same for the other two that is 14.88% and 14.81%.

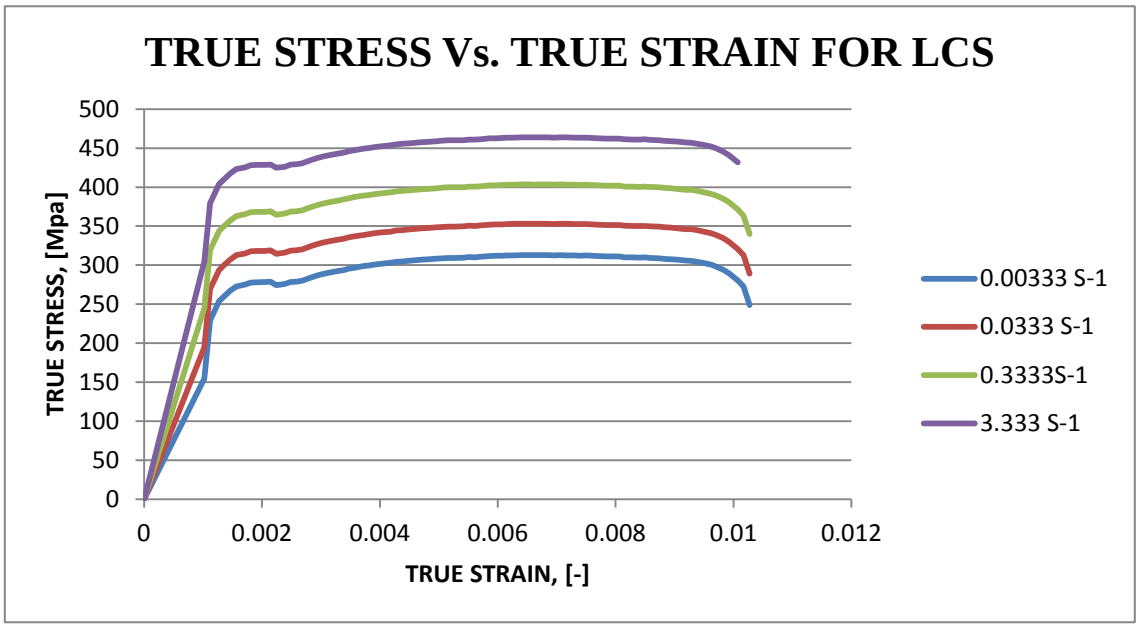

LCS = Low Carbon Steel

Figure 31 shows true stress vs. true strain at different strain rate for Steel-3

The test result of material two is shown below in figure? as true stress Vs. True strain. here the percentage increase in true stress shows the same as that for the material one as the true strain increases at the four strain rate range but slight increases of the percentage increase for material two considered here in which for the first two curves a 22.65 % increase is observed.

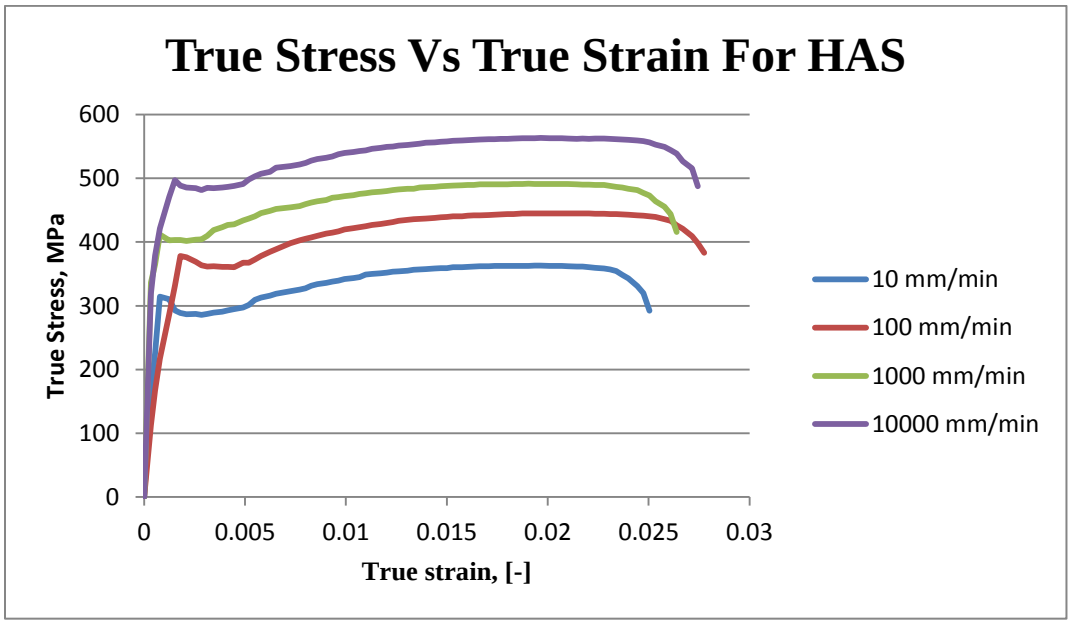

HAS = High Carbon Steel

Figure 32 shows true stress vs. true strain at different strain rate for Steel-2

The figure below illustrates that true stress vs. true strain for material one but here unlike the two the increase in true stress is less compared to the two material test results as discussed above and it is 6% for the first two strain rates.

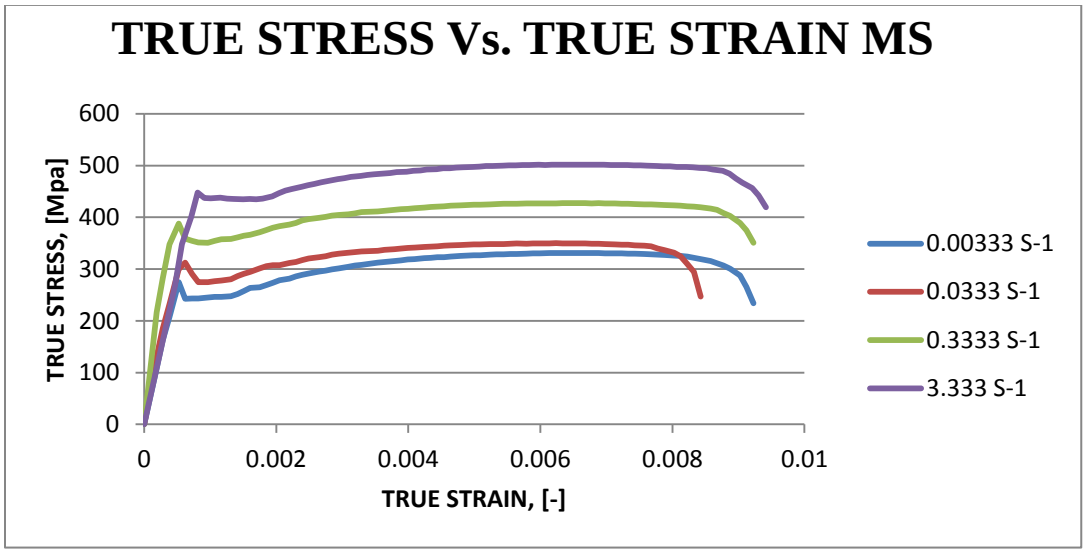

Figure 33 show the true stress vs true strain at different strain rate for steel-1, MS= Mild Steel

The lowest strain rate taken for this study is 0.00333 s^{-1} according to the graph shown below material-2 has better feature and has the maximum yield stress and Ultimate tensile strength.

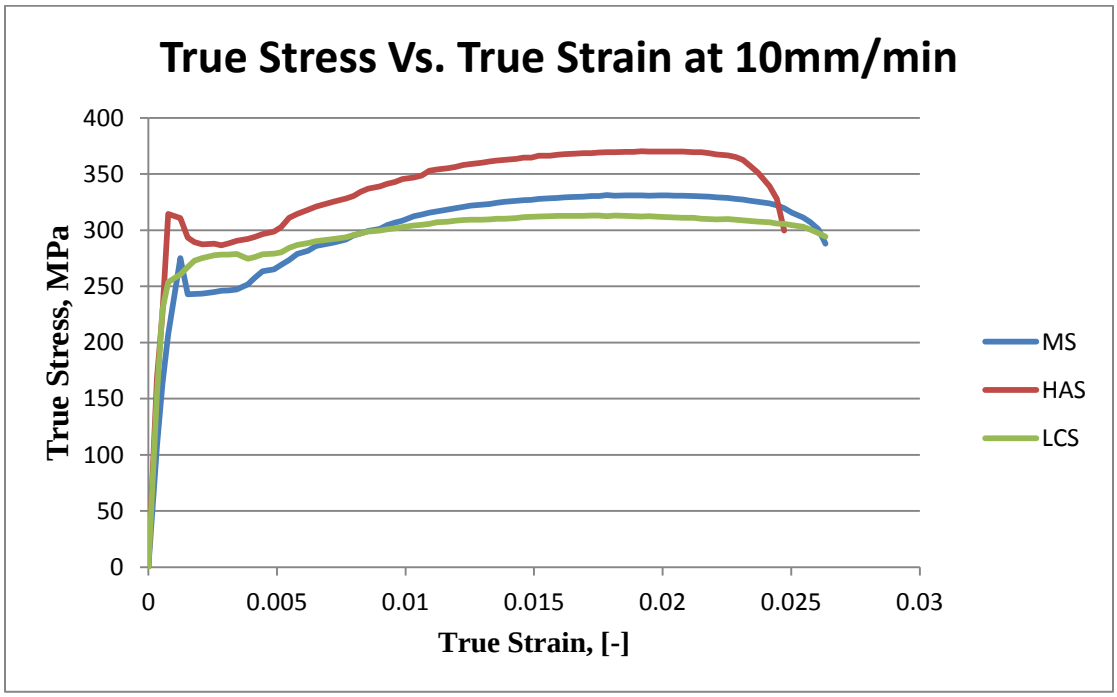

Figure 34 shows the true stress vs true strain for the three materials at 0.00333 S^{-1} strain rate

The figure from 34 through 36 indicates that the relation between true stress vs true strain which are the experimental results from the tensile test with different cross head speed of 100, 1000, and 10000 mm/min. From all the true stress vs true strain curves stated below material-2 has the maximum true ultimate strength as well as maximum yield strength for all strain rate used during the tensile test .

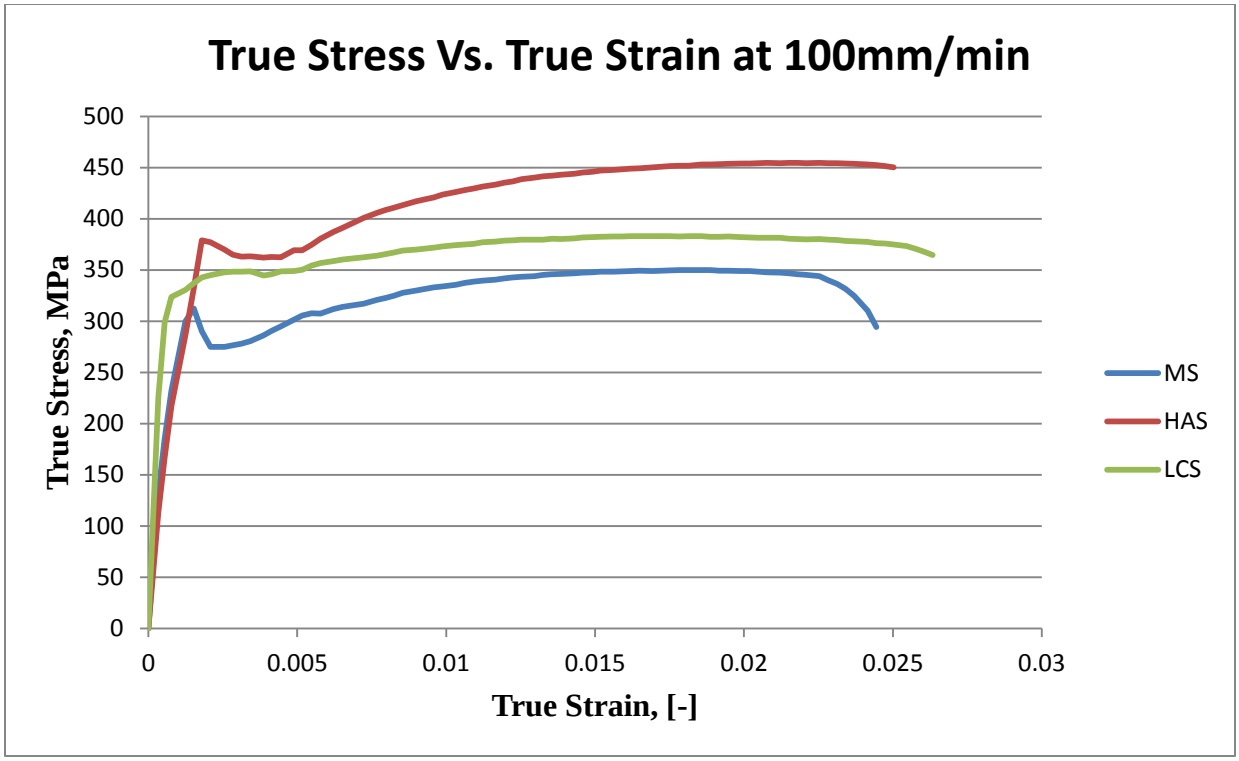

Figure 35 shows the true stress vs true strain for all three materials at 0.0333 S^{-1} strain rate

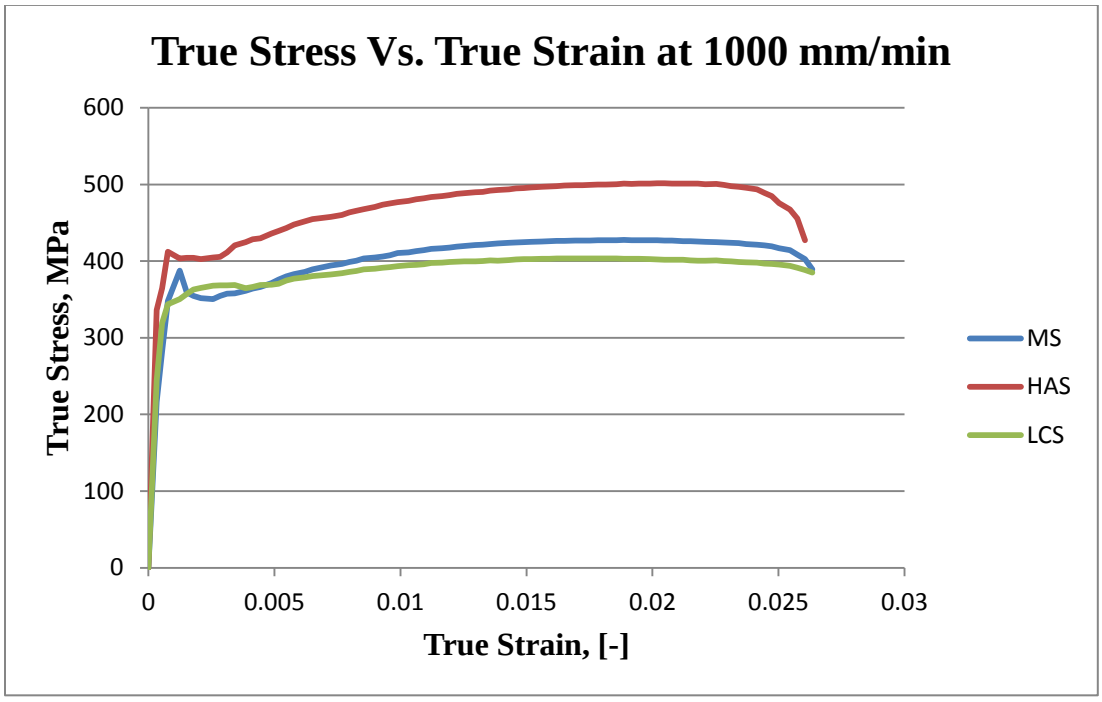

Figure 36 shows the true stress vs true strain for all three materials at 0.333 S^{-1} strain rates

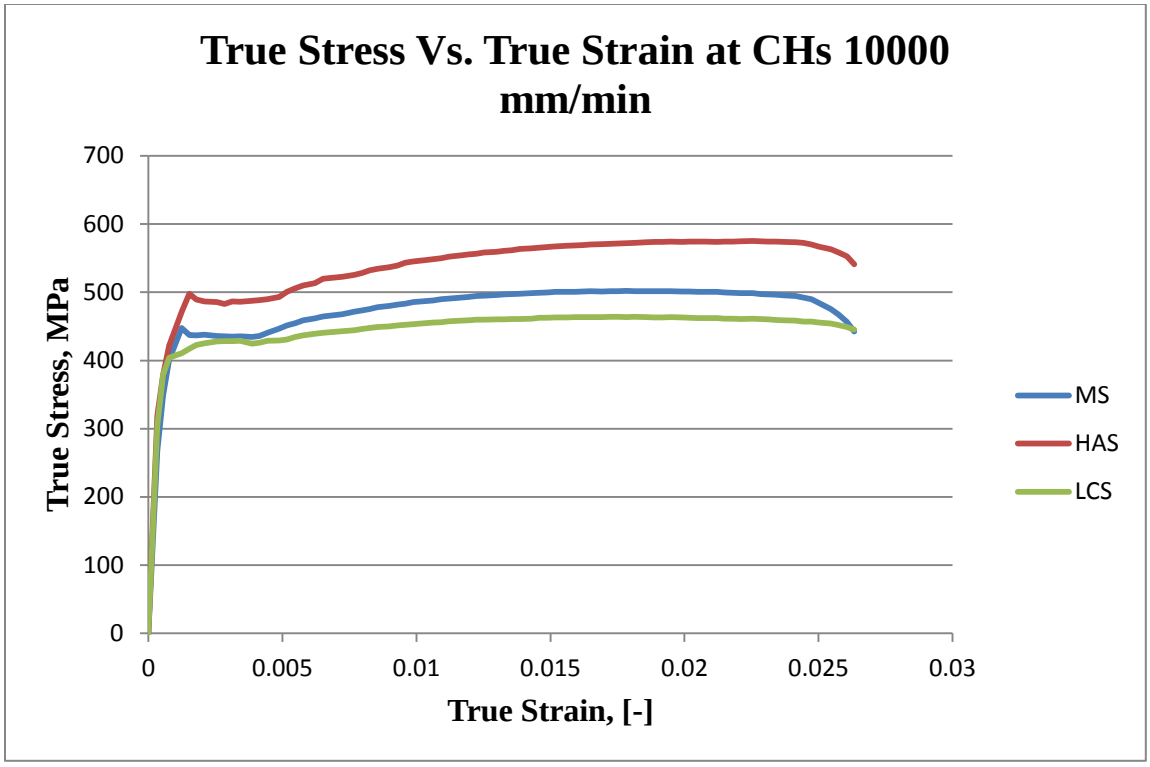

shows the true stress vs true strain for all three materials at 3.33 S^{-1} strain rate

The mean ultimate stress of the three material is shown below to judge which material among the three has the better MUTS and standard deviation of the materials under investigation the result here shows that material two has better MUTS and also from this result it is observed that as the strain rate increases the UTS strength will increases progressively when it and the error bar for each

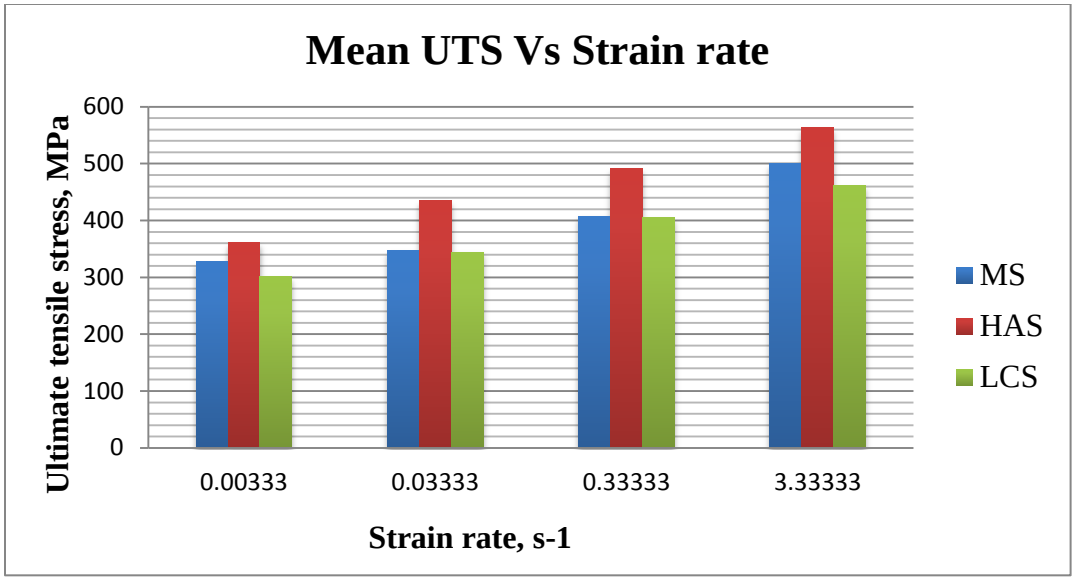

MS= Mild Steel, HAS=High Alloy Steel, LCS= Low Carbon Steel

Figure 37 shows Mean UTS vs strain rate for the three sample steel materials

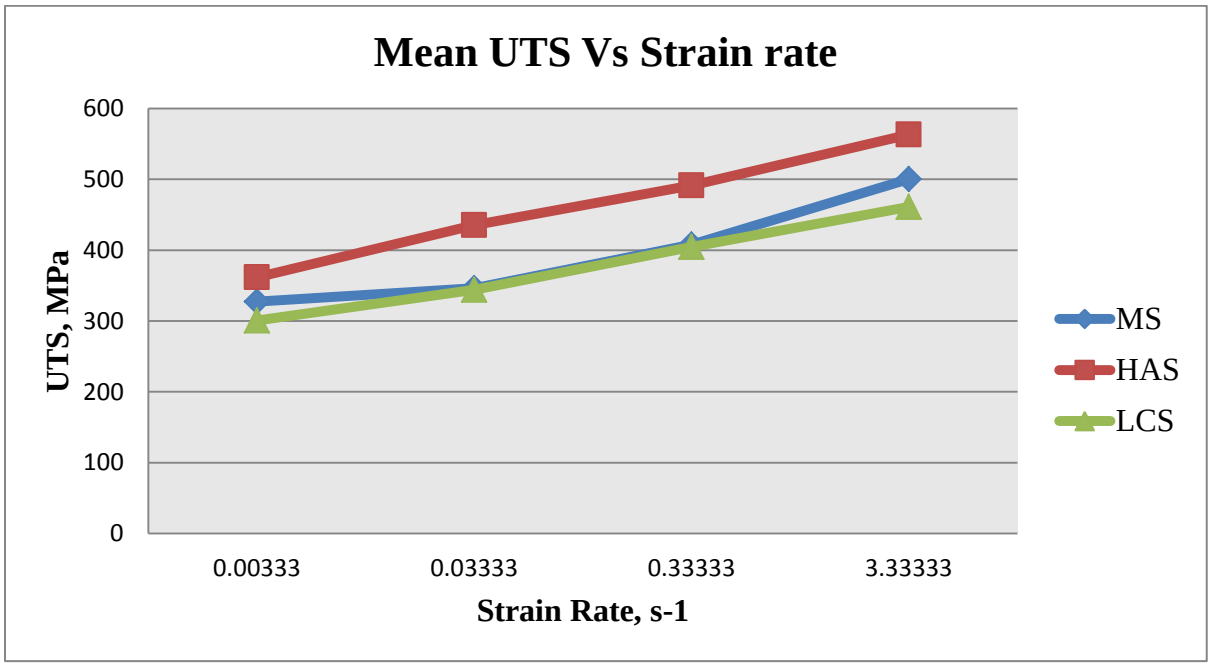

Figure 38 show UTS vs strain rate for the three materials at four different strain rate

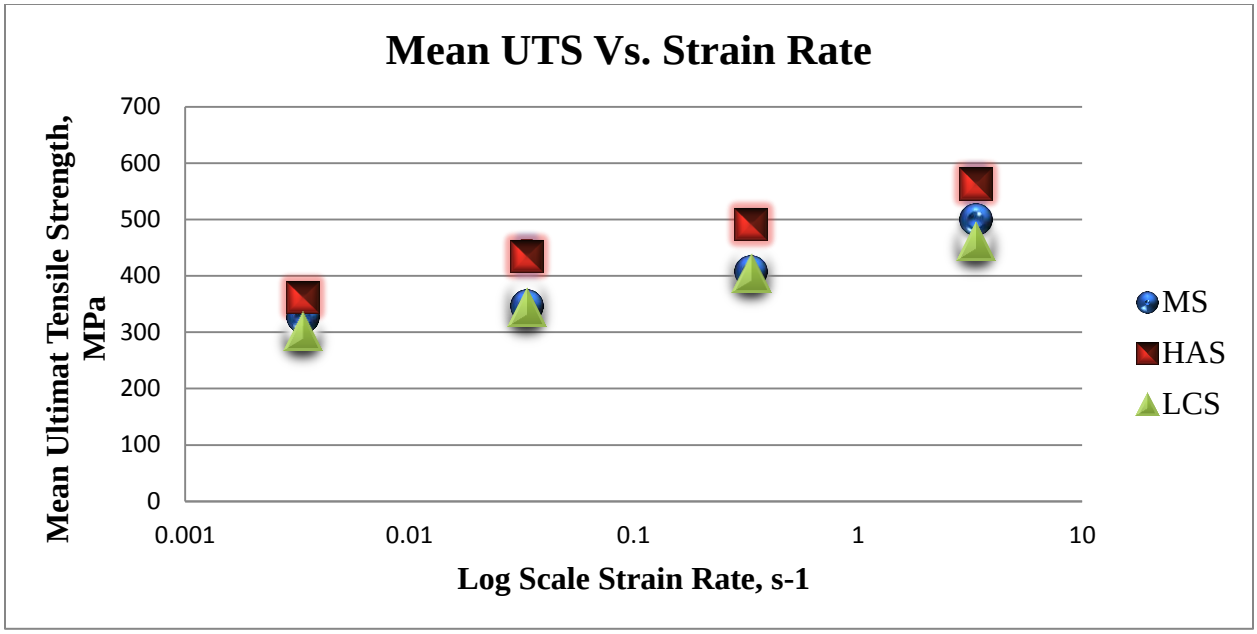

Figure 39 shows the Mean UTS vs strain rate for the three materials

4.2. FEM/ABAQUS/CAE/– Explicit Analysis Result

4.2.1. Dog bone Specimen Simulation

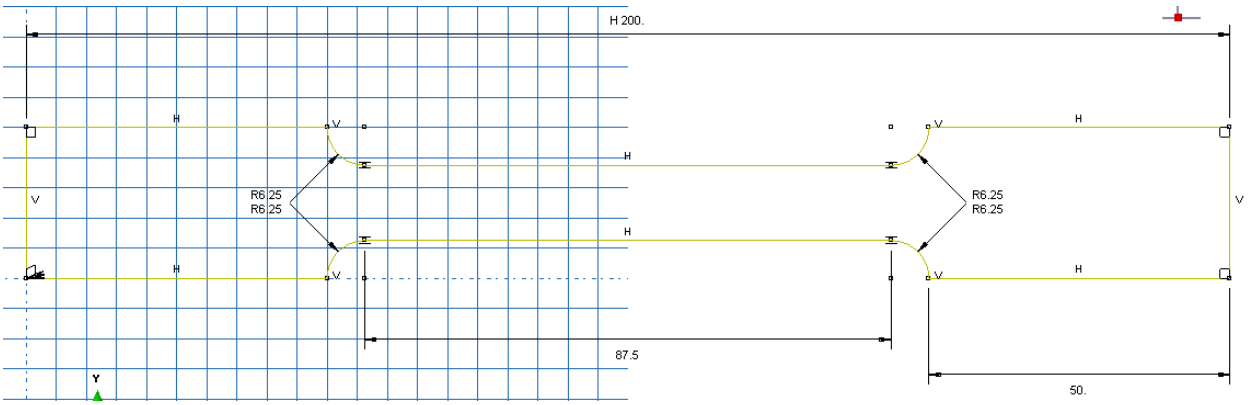

Figure 40 The 2D sketch of the specimen ABAQUS/CAE

4.2.2. Specimen 3D Geometry

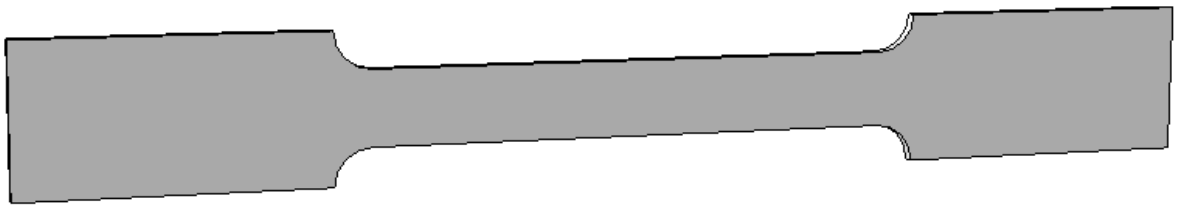

Figure 41 The extruded in 2mm thickness specimen model on ABAQUS/CAE

4.2.3. Specimen Meshing in ABAQUS Code

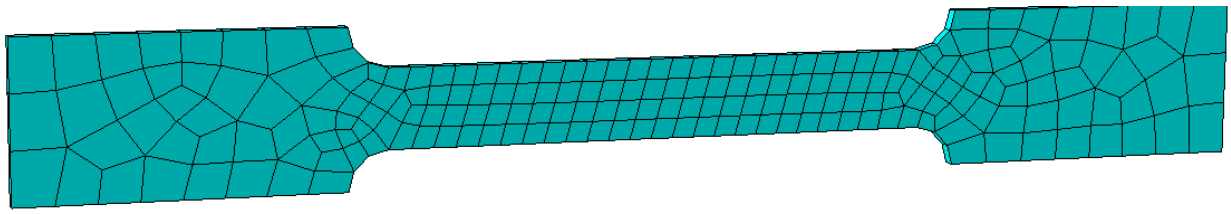

Figure 42 the specimen with a fine mesh along the gage length where measurements are taken during tensile test

4.2.4. Test result with Different Loading Rate

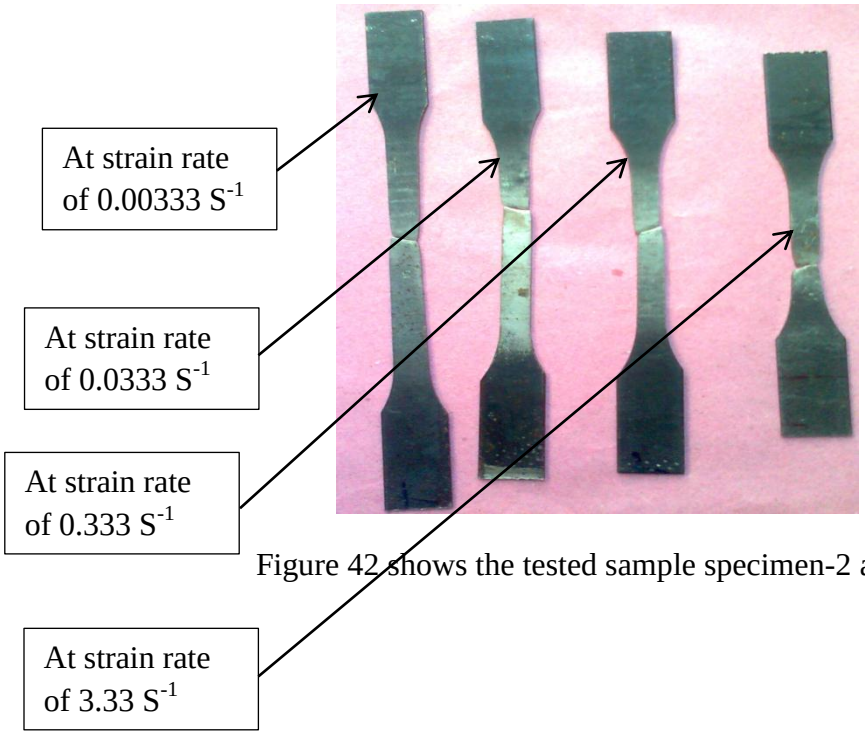

Figure 42 shows the tested sample specimen-2 after fracture for different speed

4.2.5. Three specimens test results with the same speed

Figure 43 Sample test result for the three materials at the same strain rate.

4.2.4. Counter Plot of the Results

4.2.4.1. Von Misses stress

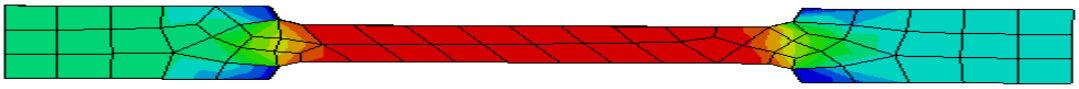

Figure 43 shows the Von misses stress counter plot result from ABAQUS Visualization module

4.2.4.2. Displacement

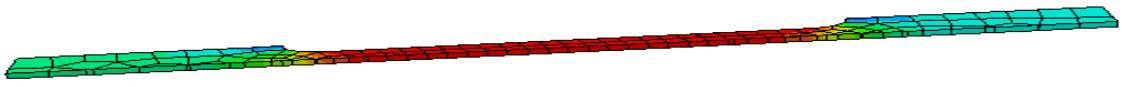

Figure 44 shows the offset cut counter plot for the displacement

4.2.4.3. The deformation or the Strain Counter

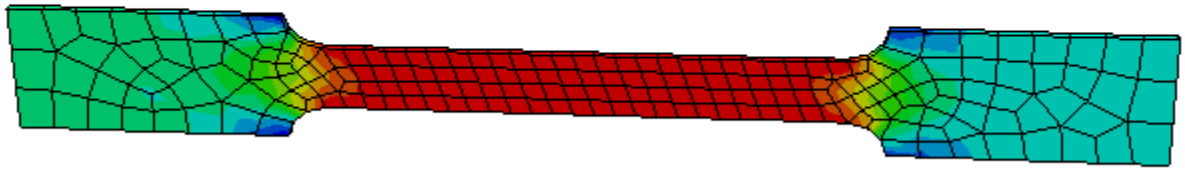

Figure 45 shows the strain couter plot for the specimen

4.2.2. The Bumper subsystem ABAQUS/CAE Result

4.2.2.1. Velocity

4.2.2.2. Displacement Magnitude

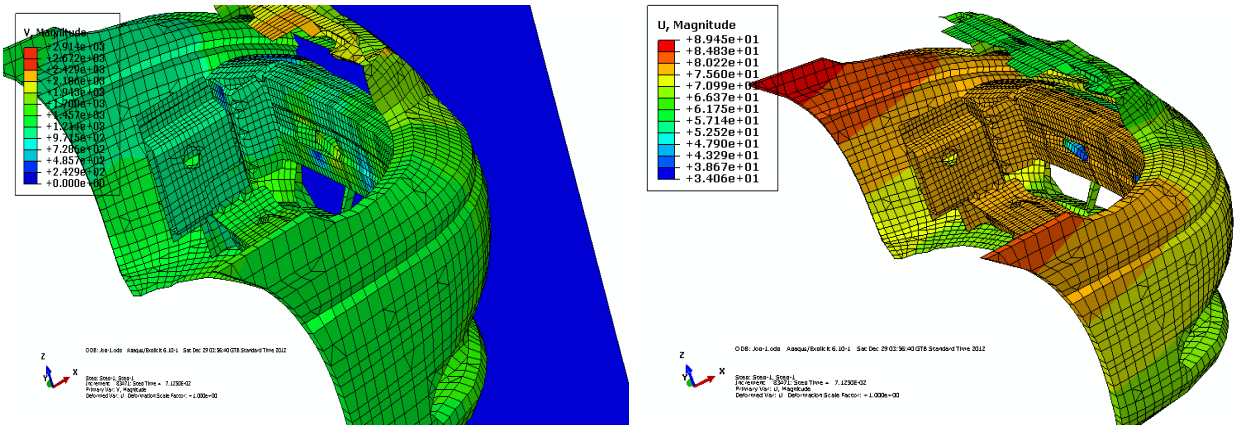

Figure 46 shows the Velocity and the displacement counter plot for the whole bumper system

4.2.2.3. Bumper Beam Displacement

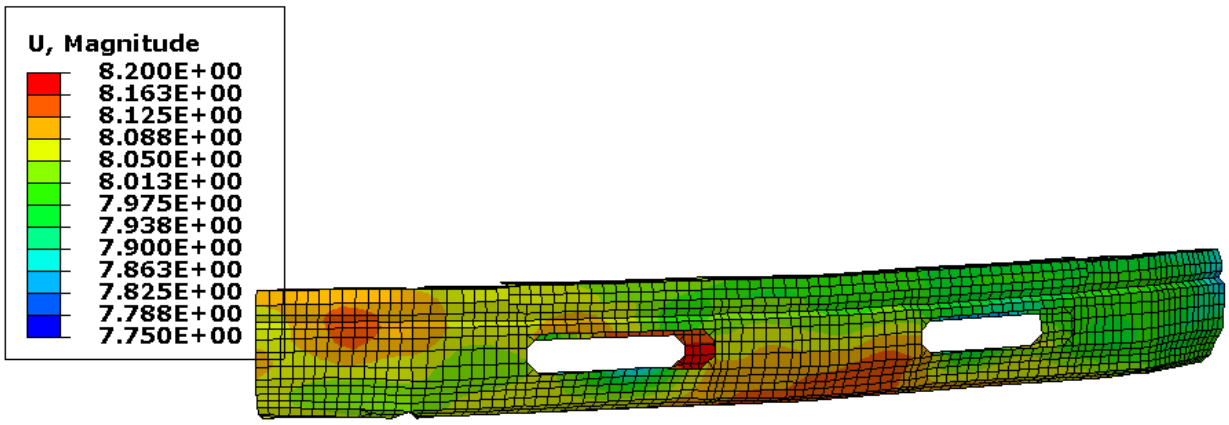

Figure 47 shows the displacement counter for the bumper beam and the foam

4.2.2.4. The Displacement Plot from ABAQUS/CAE Visualization Module

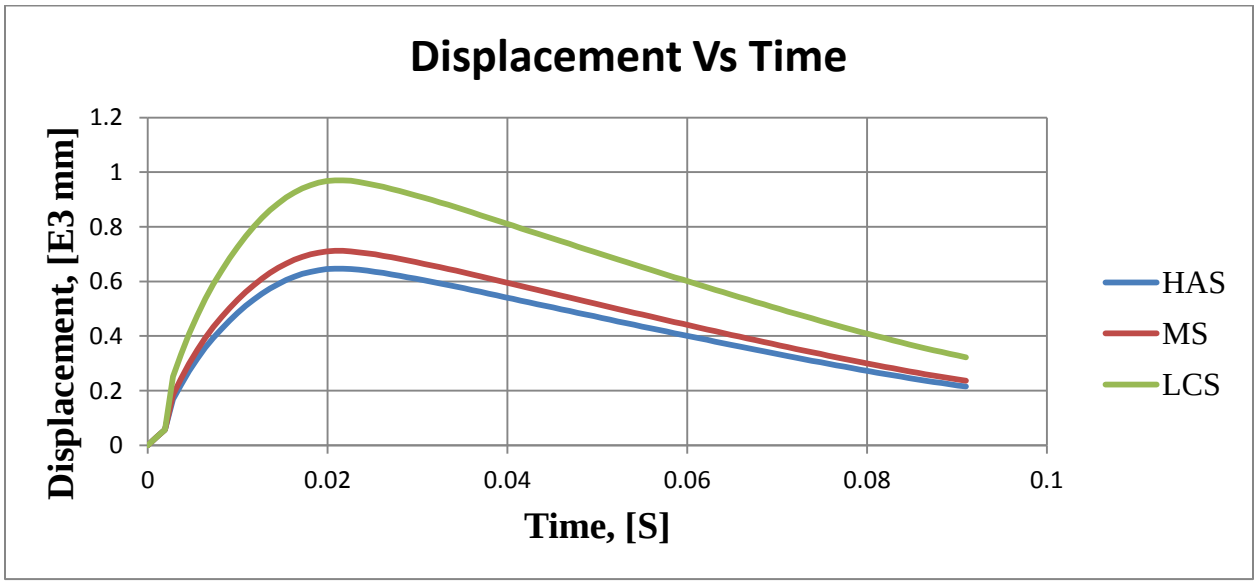

Figure 48 the displacement vs time for the bumper subsystem for the three steel materials

Figure 47 above shows a comparison of the displacement history among the three considered bumpers materials. This displacement gives a measure of the interference motion of the bumper

subsystem into the engine compartment. The reported displacement is measured at the center of gravity of the car to take in to account the global response of the vehicle due to materials and different strain rate change on bumper beam. The maximum and minimum displacements occurred in the case of steel Material three and steel Material two bumper beam, respectively. Material two solutions show minimum deflection.

Finally figure 7 shows the time diagram of the strain energy absorbed by the bumper in the three Considered material solutions. It can be noted that the highest strain energy value for each material type occurred at the highest deflection. The bumper will stretch and deform until maximum if the collision still occurs. If the energy turns to zero energy, it will become elastic collision, however according to Figure 7, minor strain energy is remained exist. This can be explained mainly by plastic deformation of energy absorber, somehow, bumper beam with material two at the maximum energy.

4.2.2.5. The Strain-Energy plot from the ABAQUS/CAE Visualization

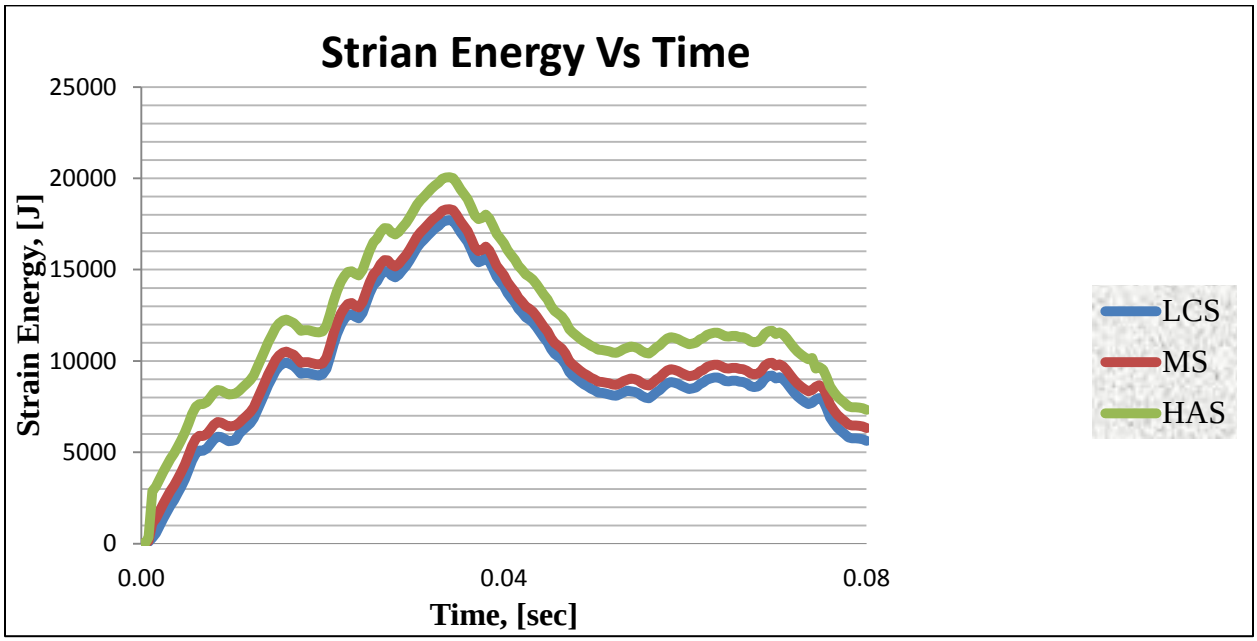

Figure 49 show the strain energy vs time for the three sample steel material

5. Conclusion and Recommendation

5.1. Conclusion

In this study three different materials-namely low carbon steels (mat-1, mat-2, and mat-3) have been evaluated for the bumper beam, to understand the effect of strain rate on a crash behavior of automobile during low speed frontal crash test performed by 36-sample specimen test in the experiment for tension at different strain rate and the data used as input to numerical simulation with ABAQUS code.

To study the steel material for bumper beam, two different factors are considered; strain rate and material type.

When the materials are tested under different strain rate for their mechanical behaviors such as yield stress and ultimate tensile strength it is observed that both the yield stress and mean UTS of the material shows positive response with the strain rate; as the strain rate increases the mean yield stress and the mean UTS increases. And material two shows 20% increase in its UTS and 14% of its yield strength when compared to the other two steel material. Hence from the experimental result material-2 improves the crash worthiness and shows better mechanical responses for such application relative to the other two materials under investigation.

On the other hand from the FEM the ABAQUS/CAE result the displacement and strain energy are plotted against the time during low speed impact of the bumper subsystem for the three low carbon steel. Material-2 absorbs more energy and shows low deformation or has the minimum displacement when it applied with dynamic loading and from this for this quasi-static strian rate material-2 has best mechanical behavior as compared to the other two steel materials for this low speed impact.

5.2. Recommendation

In this paper there are different works that are not considered and recommended for the future task as follows:

- ♠ The universal testing machine it is better if it is calibrated before testing sample specimens
- ♠ It better if thickness is considered as a factor and study its effect on vehicle weight, energy absorption and fuel consumption for bumper beam
- ♠ Effect of strain rate on steel materials comparing with composite material should be given emphasis.
- ♠ It is better if strain rate effect on both steel the reference material and composite materials are done in the future automotive crashworthiness related studies
- ♠ Material replacement is one another research currently given attention in the automation industry with the reference materials like steel with composite
- ♠ Thickness optimization using composite materials considering the same stiffness as the reference materials
- ♠ Dynamic load for medium and high speed collision under medium and high strain rate using experiment and numerical methods should be given much consideration
- ♠ Also the author recommend that it is better if during bumper beam design different cross sectional profiles are considered for better crashworthiness application
- ♠ Analysis of high strain rate and high temperature effect on the dynamic impact of vehicle bumper subsystem using the Johnson-Cook material model should be given greater attention

Reference

[1]. A, S.D., 1999. Steel bumper systems for passenger car and Light Trucks. *Sae Technical paper series*.

[2]. American Iron and Steel Institute, 2006. *Steel Bumper System For Passengers Vehicles and Light Tracks*. Report. Southfield, Michigan 48075: American Iron and Steel Institute American Iron and Steel Institute.

[3]. American Iron And Steel Institute, 2006. *Steel Bumper Systems for Passenger Cars and Light Trucks*. Report. American Iron And Steel Institute.

[4]. Association, E.A., 2011. *Case Study:Crash Management System (CMS)*. Case Study. European Aluminium Association.

[5]. Aziz, M.A.B.A., 2006. *Optimizing the stiffness and strength in bumper beam design*. Bachelor. kolej universiti Tekinikal Kebangsaan Malaysia.

[6]. Calienciug, A. & Radu, G.N., 2012. DESIGN AND FEA CRASH SIMULATION FOR A COMPOSITE CAR BUMPER. *Bulletin of the Transilvania University of Braşov*, 5(54), pp.1-12.

[7]. Chia, C.W. et al., 2007. Inverse effect of strain rate on mechanical behavior and phase transformation of superaustenitic stainless steel. *Scripta Materialia*, pp.717-20.

[8]. Coffey, C.S. & DeVost, V.F., 1986. Drop weight impact machines: a review of recent progress. In Ramesh, K.T., ed. *JANNAF Propulsion Systems Hazards Subcommittee Meeting.*, 1986. CPIA Publ.

[9]. Council, A.C., 2010-2013. *Automotive Plastic*. [Online] (2) Available at: http://www.plastics-car.com/bumpers [Accessed 29 January 2013].

[10]. Fiat, R., 2004. *The Research Requirment of the Transport Sector to Facilitate an Increased Usage of Composite Materials*. [Online] (Part II) Available at: www.compositn.net [Accessed 10 Dec 2012].

[11]. Field, J.E., 2004. Review of experimental techniques for high rate deformation and shock studies. *Int. J.Imp. Eng*, (30), p.725–775.

[12]. Hambali, A., Rabiatul, A.R., Rahim, A. & Taufik, 2012. Design Optimization Of Automotive Bumper Beam Through Energy Absorption Analysis. *International Journal of Engineering and Science*, III(2086-3799), pp.20-27.

[13]. Koricho, E.G., Martorana, B. & Belingardi, G., 2011. Design Optimization and implementation of composite and Recyclable Thermoplastic Materials for Automotive Bumper. In Koricho, Belingardi & Martorana, eds. *Fifth International Conference on Advanced Computational Methods in Engineering (ACOMEN 2011)*. Liege, 2011. University of Liege.

[14]. Luecke , E. et al., 2005. *Federal Building and Fire Safety Investigation of the World Trade Center Disaster Mechanical Properties of Structural Steels*. For Public Comment. Washington, DC: U.S. Department of Commerce Carlos M. Gutierrez, Secretary National Institute of Standards and Technology.

[15]. M. VURAL, D. RITTEL & G. RAVICHANDRAN, 2003. Large Strain Mechanical Behavior of 1018 Cold-Rolled Steel over a Wide Range of Strain Rates. *METALLURGICAL AND MATERIALS TRANSACTIONS*, 34A(A), pp.2873-85.

[16]. Malequ, M.A., Sapuan, S.M. & Suddin, N., 2012. Effect of the Strengthened Ribs in Hybrid Toughened Kenaf/ Glass Epoxy Composite Bumper Beam. *Life Science Journal*, 9(1), pp.210-13.

[17]. martins, J., 2009. *Wikipedia the free Encyclopedia*. [Online] (Latest) Available at: http://en.wikipedia.org/wiki/Bumper_(automobile) [Accessed 24 December 2012].

[18]. R. R. Balokhonov, S. Schmauder & V. A. Romanova, 2009. Finite-element and finite-difference simulations of the mechanical behavior of austenitic steels at different strain rates and temperatures. *ELSEIVER*, II(41), p.1277–1287.

[19]. Ramon-Villalonga, L. & Enderich, T., 2007. *Advanced Simulation Techniques for Low Speed Vehicle Impacts*. LS-DYNA Anwenderforum. Russelsheim: Adam Opel GmbH Frankenthal.

[20]. Rao.N.R, M.Lohrmann & L.Tall, 1996. Effect of Strain Rate on the Yield Stress of Structural Steels. *Journal of Materials*, II(1), pp.241-61.

[21]. Ravi Shriram Yatnalkar, B.E. , 2010. *Experimental Investigation of Plastic Deformation of Ti-6Al-4V under Various Loading Conditions*. Masters. Ohio: The Ohio State University The Ohio State University.

[22]. SHAH , Q., 2006. STRAIN RATE EFFECT ON THE FAILURE STRAIN AND HARDNESS OF METALLIC ARMOR PLATES SUBJECTED TO HIGH VELOCITY PROJECTILE IMPACT. *Journal of Engineering Science and Technology*, I(1), pp.166- 175.

[23]. Sierakowski, R., 1997. *STRAIN RATE BEHAVIOR OF METALS AND COMPOSITES*. MSc Thesis. Ohio USA: IGF - Cassino 27 e 28 Maggio, 1997 The Ohio State University.

[24]. Simulia, D.S., 2010. *Abaqus Analysis User's Manual*. 1st ed. Chicago: Simulia Software company.

[25]. Springer, 2008. High Strain Rate and Impact Experiments. In K.T. Ramesh, ed. *Springer Handbook of Experimental Solid Mechanics*. III ed. New York: W.N.Sharpe,Jr. pp.1-29.

[26]. Thompson, A.C., 2006. *High Strain Rate Characterization of Advanced High Strength Steels*. MSc Thesis. Ontario: University of Waterloo University of Waterloo.

[27]. Woei, S.L. & Tzay, T.S., 1997. Mechanical properties and microstructure of AISI 4340 high strength alloy steel undertempering cndition. *ELSEVIER*, pp.198-99.

[28]. http://wearanswers.com/Instant-Answers/Instant-Answers/Spark-Testing-for-Material-Identification.html

[29]. http://en.wikipedia.org/wiki/Spark_testing

Table 4 Sample Steel-1 mechanical Behavior for ABAQUS code input data

Material Name:- Steel-1		
Description:- Steel-1for Bumper beam application		
Material Behaviors		
Density		
2747 kg/m3		
Elastic		
Young's Modulus		Poisson's Ratio
2.01E+11		0.27
Plastic		
Data		
Yield Stress	Plastic Strain	Strain Rate
230	0	0
231.728	0	0.003333
245.104	0.00218654	0.003333
262.834	0.00219531	0.003333
285.396	0.00228982	0.003333
285.796	0.00229734	0.003333
288.276	0.00241828	0.003333
290.772	0.00244703	0.003333
291.955	0.00252888	0.003333
294.42	0.00254719	0.003333
296.34	0.00257039	0.003333
297.972	0.00264687	0.003333
298.452	0.00266734	0.003333
300.18	0.00268099	0.003333
303.541	0.00274687	0.003333
304.309	0.00276242	0.003333
305.514	0.00277794	0.003333
305.653	0.00286094	0.003333
307.381	0.00287302	0.003333

307.7	0.00289586	0.003333
308.629	0.00297154	0.003333
311.221	0.00299531	0.003333
312.757	0.00301039	0.003333
312.853	0.00309	0.003333
313.268	0.00310969	0.003333
314.389	0.00312099	0.003333
315.541	0.00319031	0.003333
316.436	0.00321125	0.003333
316.886	0.00322029	0.003333
317.174	0.00331023	0.003333
318.23	0.00332185	0.003333
319.382	0.00333867	0.003333
319.478	0.00342083	0.003333
319.988	0.00343875	0.003333
320.534	0.00345883	0.003333
321.302	0.00353562	0.003333
321.392	0.0035607	0.003333
321.686	0.00356943	0.003333
321.909	0.00366094	0.003333
322.005	0.0036713	0.003333
322.55	0.00376234	0.003333
322.838	0.00377154	0.003333
323.51	0	0.033333
323.798	0.00387294	0.033333
324.117	0.0038875	0.033333
324.47	0.00390812	0.033333
324.566	0.00398937	0.033333
324.95	0.00400594	0.033333
325.334	0.00401872	0.033333
325.394	0.00408883	0.033333
326.102	0.00410523	0.033333
326.142	0.00411654	0.033333
326.678	0.00420133	0.033333
326.688	0.00421583	0.033333
326.709	0.00423508	0.033333
326.966	0.00431193	0.033333
327.446	0.00433375	0.033333
327.476	0.00435125	0.033333
327.542	0.00443398	0.033333
327.638	0.00444992	0.033333
328.022	0.00446185	0.033333
328.122	0.00453164	0.033333
328.31	0.00455164	0.033333
328.406	0.00456052	0.033333

328.466	0.00465094	0.033333
328.502	0.00466224	0.033333
328.598	0.00467844	0.033333
328.6	0.00476154	0.033333
328.694	0.00478094	0.033333
328.698	0.00480125	0.033333
328.774	0.00487844	0.033333
328.79	0.00489875	0.033333
328.886	0.00491185	0.033333
329.013	0.00497844	0.033333
329.113	0.00500039	0.033333
329.174	0.00500935	0.033333
329.227	0.00508125	0.033333
330.645	0.0051	0.033333
331.893	0.00511099	0.033333
333.045	0.00517922	0.033333
334.005	0.0052106	0.033333
334.293	0.00523523	0.033333
336.213	0.00524734	0.033333
337.27	0.00533273	0.033333
337.366	0.0053457	0.033333
338.23	0.00535794	0.033333
339.286	0.00543086	0.033333
340.342	0.00544383	0.033333
341.302	0.0054563	0.033333
341.494	0.00549094	0.033333
341.878	0.00553312	0.033333
342.454	0	0.333333
342.742	0.00555443	0.333333
343.318	0.00565583	0.333333
343.606	0.00567898	0.333333
343.724	0.00569133	0.333333
344.278	0.00577828	0.333333
344.374	0.00579062	0.333333
344.662	0.00579609	0.333333
344.854	0.00580193	0.333333
345.142	0.00587812	0.333333
345.43	0.00589023	0.333333
345.814	0.00590122	0.333333
345.91	0.00597867	0.333333
346.102	0.0059982	0.333333
346.486	0.00600083	0.333333
346.489	0.00610055	0.333333
346.582	0.0061088	0.333333
346.678	0.00612445	0.333333

346.679	0.00621115	0.333333
347.062	0.00622703	0.333333
347.068	0.00622781	0.333333
347.158	0.00624898	0.333333
347.198	0.00632758	0.333333
347.35	0.00634984	0.333333
347.359	0.00635958	0.333333
347.638	0.00642508	0.333333
347.658	0.00645211	0.333333
347.678	0.00646044	0.333333
347.734	0.00653765	0.333333
347.739	0.00655258	0.333333
356.877	0.00656271	0.333333
362.734	0.00658016	0.333333
368.686	0.00666318	0.333333
371.182	0.00668008	0.333333
372.046	0.00670078	0.333333
372.91	0.00679859	0.333333
373.774	0.00681138	0.333333
373.966	0.00689758	0.333333
374.926	0.00690919	0.333333
375.022	0.0069975	0.333333
375.694	0.00700818	0.333333
375.886	0.0071457	0.333333
376.75	0.007245	0.333333
376.942	0.00725484	0.333333
377.422	0	3.33333
377.806	0.00744695	3.33333
378.286	0.0075975	3.33333
378.486	0.00771117	3.33333
378.767	0.00800203	3.33333
378.959	0.00828726	3.33333
379.535	0.00833875	3.33333
379.565	0.0084918	3.33333
380.015	0.00858281	3.33333
380.115	0.00903117	3.33333
380.399	0.0092493	3.33333
380.599	0.00932906	3.33333
380.783	0.00963375	3.33333
380.879	0.0099307	3.33333
380.975	0.0103765	3.33333
381.263	0.0106821	3.33333
381.551	0.0109828	3.33333
381.743	0.011287	3.33333
381.763	0.0117244	3.33333

381.783	0.0120178	3.33333
381.839	0.0123157	3.33333
382.031	0.012604	3.33333
382.223	0.0130537	3.33333
382.228	0.0133498	3.33333
382.253	0.0136549	3.33333
382.319	0.0139528	3.33333
382.369	0.0144038	3.33333
382.415	0.0146962	3.33333
383.465	0.0150012	3.33333
384.511	0.0153	3.33333
385.607	0.015742	3.33333
388.607	0.0160371	3.33333
415.265	0.0163315	3.33333
438.306	0.0166357	3.33333
452.419	0.017074	3.33333
463.076	0.0173719	3.33333
470.949	0.0176707	3.33333
474.021	0.0179946	3.33333
476.901	0.0183016	3.33333
478.629	0.018747	3.33333
479.877	0.0190495	3.33333
480.261	0.0193563	3.33333
481.605	0.0196577	3.33333
483.909	0.0206577	3.33333

Table 5 Sample Steel-2 Characterized with mechanical Behavior for ABAQUS code input data

Material Name:- Steel-2		
Description:- Steel-1for Bumper beam application		
Material Behaviors		
Density		
2845 kg/m3		
Elastic		
Young's Modulus		*Poisson's Ratio*
2.06E+11		*0.3*
Plastic		
Data		
Yield Stress	*Plastic Strain*	*Strain Rate*
320	*0*	*0*
321.32	*0*	*0.003333*
324.104	*0.00218654*	*0.003333*
325.064	*0.00219531*	*0.003333*
328.328	*0.00228982*	*0.003333*
330.92	*0.00229734*	*0.003333*
332.936	*0.00241828*	*0.003333*
336.585	*0.00244703*	*0.003333*
339.273	*0.00252888*	*0.003333*
341.193	*0.00254719*	*0.003333*
343.305	*0.00257039*	*0.003333*
344.937	*0.00264687*	*0.003333*
347.433	*0.00266734*	*0.003333*
348.681	*0.00268099*	*0.003333*
350.217	*0.00274687*	*0.003333*
354.154	*0.00276242*	*0.003333*
355.306	*0.00277794*	*0.003333*
356.266	*0.00286094*	*0.003333*
357.226	*0.00287302*	*0.003333*
358.858	*0.00289586*	*0.003333*
359.53	*0.00297154*	*0.003333*
360.49	*0.00299531*	*0.003333*
361.642	*0.00301039*	*0.003333*

362.314	*0.00309*	*0.003333*
362.794	*0.00310969*	*0.003333*
363.562	*0.00312099*	*0.003333*
364.426	*0.00319031*	*0.003333*
364.522	*0.00321125*	*0.003333*
365.866	*0.00322029*	*0.003333*
365.866	*0.00331023*	*0.003333*
366.442	*0.00332185*	*0.003333*
366.922	*0.00333867*	*0.003333*
367.21	*0.00342083*	*0.003333*
367.499	*0.00343875*	*0.003333*
367.595	*0.00345883*	*0.003333*
367.883	*0.00353562*	*0.003333*
367.979	*0.0035607*	*0.003333*
368.075	*0.00356943*	*0.003333*
368.075	*0.00366094*	*0.003333*
368.075	*0.0036713*	*0.003333*
368.171	*0.00376234*	*0.003333*
368.459	*0.00377154*	*0.003333*
383.028	*0*	*0.033333*
388.5	*0.00387294*	*0.033333*
398.005	*0.0038875*	*0.033333*
402.613	*0.00390812*	*0.033333*
405.301	*0.00398937*	*0.033333*
407.509	*0.00400594*	*0.033333*
409.718	*0.00401872*	*0.033333*
413.27	*0.00408883*	*0.033333*
414.998	*0.00410523*	*0.033333*
416.822	*0.00411654*	*0.033333*
419.606	*0.00420133*	*0.033333*
421.814	*0.00421583*	*0.033333*
423.446	*0.00423508*	*0.033333*
425.078	*0.00431193*	*0.033333*
426.711	*0.00433375*	*0.033333*
428.343	*0.00435125*	*0.033333*
430.071	*0.00443398*	*0.033333*
431.223	*0.00444992*	*0.033333*
433.239	*0.00446185*	*0.033333*
434.679	*0.00453164*	*0.033333*
435.735	*0.00455164*	*0.033333*

436.215	*0.00456052*	*0.033333*
436.887	*0.00465094*	*0.033333*
437.749	*0.00466224*	*0.033333*
438.711	*0.00467844*	*0.033333*
439.287	*0.00476154*	*0.033333*
440.343	*0.00478094*	*0.033333*
440.631	*0.00480125*	*0.033333*
441.4	*0.00487844*	*0.033333*
441.88	*0.00489875*	*0.033333*
442.072	*0.00491185*	*0.033333*
442.552	*0.00497844*	*0.033333*
443.032	*0.00500039*	*0.033333*
443.608	*0.00500935*	*0.033333*
443.8	*0.00508125*	*0.033333*
443.8	*0.0051*	*0.033333*
444.472	*0.00511099*	*0.033333*
444.472	*0.00517922*	*0.033333*
444.664	*0.0052106*	*0.033333*
444.664	*0.00523523*	*0.033333*
444.664	*0.00524734*	*0.033333*
444.856	*0.00533273*	*0.033333*
444.856	*0.0053457*	*0.033333*
444.856	*0.00535794*	*0.033333*
444.952	*0.00543086*	*0.033333*
444.952	*0.00544383*	*0.033333*
444.952	*0.0054563*	*0.033333*
445.144	*0.00549094*	*0.033333*
445.144	*0.00553312*	*0.033333*
445.219	*0*	*0.333333*
449.155	*0.00555443*	*0.333333*
451.843	*0.00565583*	*0.333333*
454.243	*0.00567898*	*0.333333*
456.548	*0.00569133*	*0.333333*
459.716	*0.00577828*	*0.333333*
461.828	*0.00579062*	*0.333333*
463.844	*0.00579609*	*0.333333*
466.244	*0.00580193*	*0.333333*
469.316	*0.00587812*	*0.333333*
470.565	*0.00589023*	*0.333333*
472.101	*0.00590122*	*0.333333*

473.637	*0.00597867*	*0.333333*
475.557	*0.0059982*	*0.333333*
476.517	*0.00600083*	*0.333333*
478.149	*0.00610055*	*0.333333*
479.205	*0.0061088*	*0.333333*
480.165	*0.00612445*	*0.333333*
481.701	*0.00621115*	*0.333333*
482.565	*0.00622703*	*0.333333*
483.333	*0.00622781*	*0.333333*
483.813	*0.00624898*	*0.333333*
485.349	*0.00632758*	*0.333333*
486.117	*0.00634984*	*0.333333*
486.406	*0.00635958*	*0.333333*
487.462	*0.00642508*	*0.333333*
488.038	*0.00645211*	*0.333333*
488.422	*0.00646044*	*0.333333*
488.998	*0.00653765*	*0.333333*
489.574	*0.00655258*	*0.333333*
489.766	*0.00656271*	*0.333333*
490.342	*0.00658016*	*0.333333*
490.63	*0.00666318*	*0.333333*
490.63	*0.00668008*	*0.333333*
490.63	*0.00670078*	*0.333333*
490.822	*0.00679859*	*0.333333*
491.014	*0.00681138*	*0.333333*
491.11	*0.00689758*	*0.333333*
491.206	*0.00690919*	*0.333333*
491.206	*0.0069975*	*0.333333*
491.302	*0.00700818*	*0.333333*
491.302	*0.0071457*	*0.333333*
491.302	*0.007245*	*0.333333*
491.494	*0.00725484*	*0.333333*
498.328	*0*	*3.33333*
503.128	*0.00744695*	*3.33333*
507.064	*0.0075975*	*3.33333*
510.041	*0.00771117*	*3.33333*
516.473	*0.00800203*	*3.33333*
518.969	*0.00828726*	*3.33333*
521.465	*0.00833875*	*3.33333*
524.154	*0.0084918*	*3.33333*

527.898	*0.00858281*	*3.33333*
530.01	*0.00903117*	*3.33333*
532.122	*0.0092493*	*3.33333*
534.33	*0.00932906*	*3.33333*
537.978	*0.00963375*	*3.33333*
539.803	*0.0099307*	*3.33333*
541.339	*0.0103765*	*3.33333*
542.683	*0.0106821*	*3.33333*
543.931	*0.0109828*	*3.33333*
546.331	*0.011287*	*3.33333*
547.867	*0.0117244*	*3.33333*
549.211	*0.0120178*	*3.33333*
549.979	*0.0123157*	*3.33333*
551.323	*0.012604*	*3.33333*
552.187	*0.0130537*	*3.33333*
553.531	*0.0133498*	*3.33333*
554.299	*0.0136549*	*3.33333*
555.74	*0.0139528*	*3.33333*
556.508	*0.0144038*	*3.33333*
557.276	*0.0146962*	*3.33333*
558.044	*0.0150012*	*3.33333*
558.908	*0.0153*	*3.33333*
559.292	*0.015742*	*3.33333*
559.772	*0.0160371*	*3.33333*
560.156	*0.0163315*	*3.33333*
560.828	*0.0166357*	*3.33333*
561.212	*0.017074*	*3.33333*
561.404	*0.0173719*	*3.33333*
561.692	*0.0176707*	*3.33333*
561.788	*0.0179946*	*3.33333*
562.268	*0.0183016*	*3.33333*
562.844	*0.018747*	*3.33333*
563.036	*0.0190495*	*3.33333*
563.036	*0.0193563*	*3.33333*
563.132	*0.0196577*	*3.33333*

Appendix C

Table 6 Sample Steel-3 mechanical Behavior for ABAQUS code input data

Material Name:- Steel-3		
Description:- Steel-1for Bumper beam application		
Material Behaviors		
Density		
2845 kg/m3		
Elastic		
Young's Modulus		Poisson's Ratio
2.06E+11		0.3
Plastic		
Data		
Yield Stress	Plastic Strain	Strain Rate
230.000000000	0.000000000	0.000000000
231.728085900	0.000000000	0.003333000
245.103632800	0.002300000	0.003333000
262.834082000	0.002312000	0.003333000
285.395527300	0.002396092	0.003333000
285.395527300	0.002396127	0.003333000
288.275722700	0.002495624	0.003333000
290.771875000	0.002495625	0.003333000
291.954687500	0.002649607	0.003333000
294.420117200	0.002649608	0.003333000
296.340234400	0.002750701	0.003333000
297.972324200	0.002750702	0.003333000
298.452363300	0.002850600	0.003333000
300.180488300	0.002850624	0.003333000
303.540683600	0.002950300	0.003333000
304.308710900	0.002950312	0.003333000
305.513849700	0.003037804	0.003333000
305.652832000	0.003098421	0.003333000
307.380918000	0.003098436	0.003333000
307.699687500	0.003137492	0.003333000
308.628984400	0.003197320	0.003333000
311.221210900	0.003197420	0.003333000
312.757265600	0.003285616	0.003333000

312.853320300	0.003296250	0.003333000
313.268007800	0.003299250	0.003333000
314.389414100	0.003384600	0.003333000
315.541445300	0.003483430	0.003333000
316.436230500	0.003546012	0.003333000
316.885507800	0.003546014	0.003333000
317.173554700	0.003644354	0.003333000
318.229648400	0.003644374	0.003333000
319.381679700	0.003733194	0.003333000
319.477734400	0.003796301	0.003333000
319.988437500	0.003796328	0.003333000
320.533750000	0.003831554	0.003333000
321.301796900	0.003892792	0.003333000
321.391796900	0.003895301	0.003333000
321.685859400	0.003895312	0.003333000
321.908593800	0.003983508	0.003333000
322.004609400	0.004000058	0.003333000
322.549921900	0.004002567	0.003333000
322.837929700	0.004002578	0.003333000
323.510000000	0.004082492	0.003333000
323.798007800	0.004100604	0.003333000
324.116757800	0.004102124	0.003333000
324.470000000	0.004103124	0.003333000
324.566054700	0.004189758	0.003333000
324.950039100	0.004247870	0.003333000
325.334062500	0.004250390	0.003333000
325.394062500	0.004250490	0.003333000
326.102109400	0.004290304	0.003333000
326.142109400	0.004347166	0.003333000
326.678203100	0.004349586	0.003333000
326.688203100	0.004349686	0.003333000
326.708886700	0.004437570	0.003333000
326.966210900	0.004447400	0.003333000
327.446210900	0.004448920	0.003333000
327.476210900	0.004449920	0.003333000
327.542226600	0.004536866	0.003333000
327.638242200	0.004548182	0.003333000
328.022226600	0.004550302	0.003333000
328.122226600	0.004550702	0.003333000
328.310273400	0.004637100	0.003333000
328.406289100	0.000000000	0.033330000
328.466289100	0.004651734	0.033330000
328.502265600	0.004652734	0.033330000
328.598320300	0.004737882	0.033330000
328.599720300	0.004798104	0.033330000

328.694335900	0.004800600	0.033330000
328.698335900	0.004800624	0.033330000
328.774335900	0.004839914	0.033330000
328.790273400	0.004899042	0.033330000
328.886328100	0.004900562	0.033330000
329.013046900	0.004901562	0.033330000
329.113046900	0.004987804	0.033330000
329.174335900	0.005001308	0.033330000
329.227326300	0.005001828	0.033330000
330.645117200	0.005003828	0.033330000
331.893242200	0.005088742	0.033330000
333.045273400	0.005100292	0.033330000
334.005351600	0.005101812	0.033330000
334.293359400	0.005102812	0.033330000
336.213476600	0.005191008	0.033330000
337.269570300	0.005252558	0.033330000
337.365546900	0.005255078	0.033330000
338.229648400	0.005255178	0.033330000
339.285664100	0.005289992	0.033330000
340.341757800	0.005350058	0.033330000
341.301796900	0.005352478	0.033330000
341.493789100	0.005352578	0.033330000
341.877851600	0.005442258	0.033330000
342.453867200	0.005454744	0.033330000
342.741914100	0.005457064	0.033330000
343.317968800	0.005457264	0.033330000
343.605976600	0.005539758	0.033330000
343.724279400	0.005555838	0.033330000
344.278007800	0.005558058	0.033330000
344.374023400	0.005558358	0.033330000
344.661992200	0.005644444	0.033330000
344.854023400	0.005656072	0.033330000
345.142070300	0.005658192	0.033330000
345.430078100	0.005658592	0.033330000
345.814101600	0.005745538	0.033330000
345.910117200	0.005805760	0.033330000
346.102109400	0.005808280	0.033330000
346.486171900	0.005818280	0.033330000
346.489171900	0.005845772	0.033330000
346.582148400	0.005903964	0.033330000
346.678203100	0.005906484	0.033330000
346.679203100	0.005936484	0.033330000
347.062187500	0.005995460	0.033330000
347.068187500	0.006004354	0.033330000
347.158242200	0.006006874	0.033330000

347.198242200	0.006046874	0.033330000
347.350195300	0.006093664	0.033330000
347.359195300	0.006152558	0.033330000
347.638242200	0.006155078	0.033330000
347.658242200	0.006155278	0.033330000
347.678242200	0.000000000	0.333300000
347.734257800	0.006253104	0.333300000
347.739257800	0.006255624	0.333300000
356.877111400	0.006257624	0.333300000
362.733517700	0.006342258	0.333300000
368.685920000	0.006352714	0.333300000
371.182052800	0.006355234	0.333300000
372.046076300	0.006355634	0.333300000
372.910138800	0.006442804	0.333300000
373.774240300	0.006451386	0.333300000
373.966193400	0.006453906	0.333300000
374.926271600	0.006454906	0.333300000
375.022287200	0.006542414	0.333300000
375.694318400	0.006551308	0.333300000
375.886310600	0.006553828	0.333300000
376.750412200	0.006563828	0.333300000
376.942443400	0.006641086	0.333300000
377.422443400	0.006697088	0.333300000
377.806427800	0.006699608	0.333300000
378.286466900	0.006699708	0.333300000
378.486466900	0.006741008	0.333300000
378.766505900	0.006793964	0.333300000
378.958576300	0.006796484	0.333300000
379.534552800	0.006799484	0.333300000
379.564552800	0.006886788	0.333300000
380.014591900	0.006901698	0.333300000
380.114591900	0.006924218	0.333300000
380.398654400	0.006904218	0.333300000
380.598654400	0.006983664	0.333300000
380.782638800	0.007001230	0.333300000
380.878693400	0.007003750	0.333300000
380.974630900	0.007043750	0.333300000
381.262677800	0.007091398	0.333300000
381.550724700	0.007153964	0.333300000
381.742716900	0.007156484	0.333300000
381.762716900	0.007159484	0.333300000
381.782716900	0.007190930	0.333300000
381.838732500	0.007252714	0.333300000
382.030763800	0.007255234	0.333300000
382.222716900	0.007295234	0.333300000

382.227716900	0.007343664	0.333300000
382.252716900	0.007354354	0.333300000
382.318771600	0.007356874	0.333300000
382.368771600	0.007396874	0.333300000
382.414709100	0.007442414	0.333300000
382.464709100	0.007453964	0.333300000
382.510802800	0.007456484	0.333300000
382.606779400	0.007459484	0.333300000
382.606779400	0.007544054	0.333300000
415.264960900	0.000000000	3.333300000
438.306406300	0.007605624	3.333300000
452.419316400	0.007625624	3.333300000
463.075996100	0.007643664	3.333300000
470.948515600	0.007704744	3.333300000
474.020722700	0.007717264	3.333300000
476.900918000	0.007737264	3.333300000
478.628984400	0.007792804	3.333300000
479.877070300	0.007804354	3.333300000
480.261132800	0.007806874	3.333300000
481.605195300	0.007846874	3.333300000
483.909375000	0.007894444	3.333300000
485.445429700	0.007906698	3.333300000
485.745429700	0.007909218	3.333300000
486.309531300	0.007959218	3.333300000
487.845585900	0.007994054	3.333300000
488.133593800	0.008055214	3.333300000
488.613632800	0.008057734	3.333300000
490.149765600	0.008077734	3.333300000
490.437773400	0.008096398	3.333300000
490.917812500	0.008153886	3.333300000
491.493789100	0.008156406	3.333300000
492.357929700	0.008159406	3.333300000
492.557929700	0.008244914	3.333300000
492.741914100	0.008255604	3.333300000
493.029960900	0.008258124	3.333300000
493.605976600	0.008278124	3.333300000
493.798007800	0.008343586	3.333300000
494.470000000	0.008360604	3.333300000
494.758085900	0.008363124	3.333300000
494.950039100	0.008369124	3.333300000
495.046054700	0.008445304	3.333300000
495.430078100	0.008460760	3.333300000
495.430978100	0.008463280	3.333300000
495.814101600	0.008465280	3.333300000
496.390117200	0.008550304	3.333300000

496.678203100	0.008612558	3.333300000
496.870156300	0.008615078	3.333300000
496.966210900	0.008650460	3.333300000
497.254218800	0.008712480	3.333300000
497.354218800	0.008715000	3.333300000
497.542226600	0.008802258	3.333300000
497.830195300	0.008809980	3.333300000
497.839195300	0.008812500	3.333300000
497.930195300	0.008902180	3.333300000
498.022226600	0.008910760	3.333300000
498.092226600	0.008913280	3.333300000
498.118281300	0.008999680	3.333300000
498.214257800	0.009060214	3.333300000
498.310273400	0.009062734	3.333300000
498.390273400	0.009100460	3.333300000
498.406289100	0.009160682	3.333300000
498.446289100	0.009163202	3.333300000
498.598320300	0.009249914	3.333300000
498.599320300	0.009270136	3.333300000
498.694335900	0.009350382	3.333300000
498.790273400	0.009459836	3.333300000

Table 7 Foam Material Properties for ABAQUS/CAE as an input

Material Name:- Foam		
Description:- Foam material for energy absorber		
Mass Density	Elastic	
8.32E-011 kg/m3	Young's Modulus	Poisson's Ratio
	25	0.3
Plastic		
Crushable Foam		
Compression Yield Stress Ratio	Plastic Poisson's Ratio	
0.99995	0	
Crushable Foam Hardening		
Yield Stress	Uniaxial Plastic Strain	
0.1659	0	
0.2805	0.0206	
0.3597	0.0417	
0.4308	0.0632	
0.4908	0.0852	
0.5442	0.1076	
0.5908	0.1306	
0.6224	0.1542	
0.654	0.1783	
0.6724	0.2029	
0.6921	0.2283	
0.7101	0.2542	
0.7231	0.2809	
0.7294	0.3083	
0.7411	0.3365	
0.7453	0.3655	
0.756	0.3953	
0.7633	0.4261	
0.7685	0.4578	
0.7721	0.4907	
0.7787	0.5245	
0.7865	0.5596	
0.804	0.596	
0.8223	0.6337	
0.8461	0.6729	

0.8778	0.7138	
0.9265	0.7563	
0.9789	0.8008	
1.054	0.8473	
1.1469	0.8961	
1.253	0.9474	
1.3652	1.0015	
1.4915	1.0586	
1.6459	1.1192	
1.8331	1.1838	
2.0488	1.2528	
2.3373	1.3268	
2.7392	1.407	
3.2833	1.4939	
4.0443	1.5892	
5.1895	1.6947	
Rate Dependent		
Power Law		
Multiplier (k)	Exponent (n)	
4867	4.338	

Table 8 Plastic Property data for Plastic part of bumper subsystem Fasica input to ABAQUS/CAE

Material Name:- Plastic		
Description:- Plastic material for Fasica		
Material Behaviors		
Mass Density	Elastic	
1.20E-09	Young's Modulus	Poisson's Ratio
	2800.000000000	0.300000000
Plastic		
Yield Stress	Plastic Strian	
45	0	
885	2	

Table 9 Steel Material Property for the Rail and Crush Box as input to ABAQUS code

Material Name:- Steel		
Description:-Steel material for Rail and Crush Box		

Material Behaviors		
Mass Density	Elastic	
7.89E-09	Young's Modulus	Poisson's Ratio
	210000.000000000	0.300000000
Plastic		
Yield Stress	Plastic Strain	
300	0	
333	0.039	
367	0.077	
395	0.122	
425	0.166	
474	0.247	
550	0.322	
700	0.392	
710	1	
712.06	1.125	
714.11	1.25	
716.17	1.375	
718.22	1.5	
720.28	1.625	
722.34	1.75	
724.39	1.875	
726.45	2	

Table 10 Steel Material property data for the cooling support as input to ABAQUS/CAE

Material Name:- Steel		
Description:- Steel material for the cooling support		
Material Behaviors		
Mass Density	Elastic	
7.89E-09	Young's Modulus	Poisson's Ratio
	210000.000000000	0.300000000
Plastic		
Yield Stress	Plastic Strain	
330	0	
367	0.02	
372	0.049	
379	0.082	
380	0.127	

381	0.17	
430	0.231	
500	0.278	
510	1	
511.73	1.125	
513.46	1.25	
515.19	1.375	
516.93	1.5	
518.66	1.625	
520.39	1.75	
522.12	1.875	
523.85	2	

The paper below shows sample material sources taken from Metal and Engineering Corporations

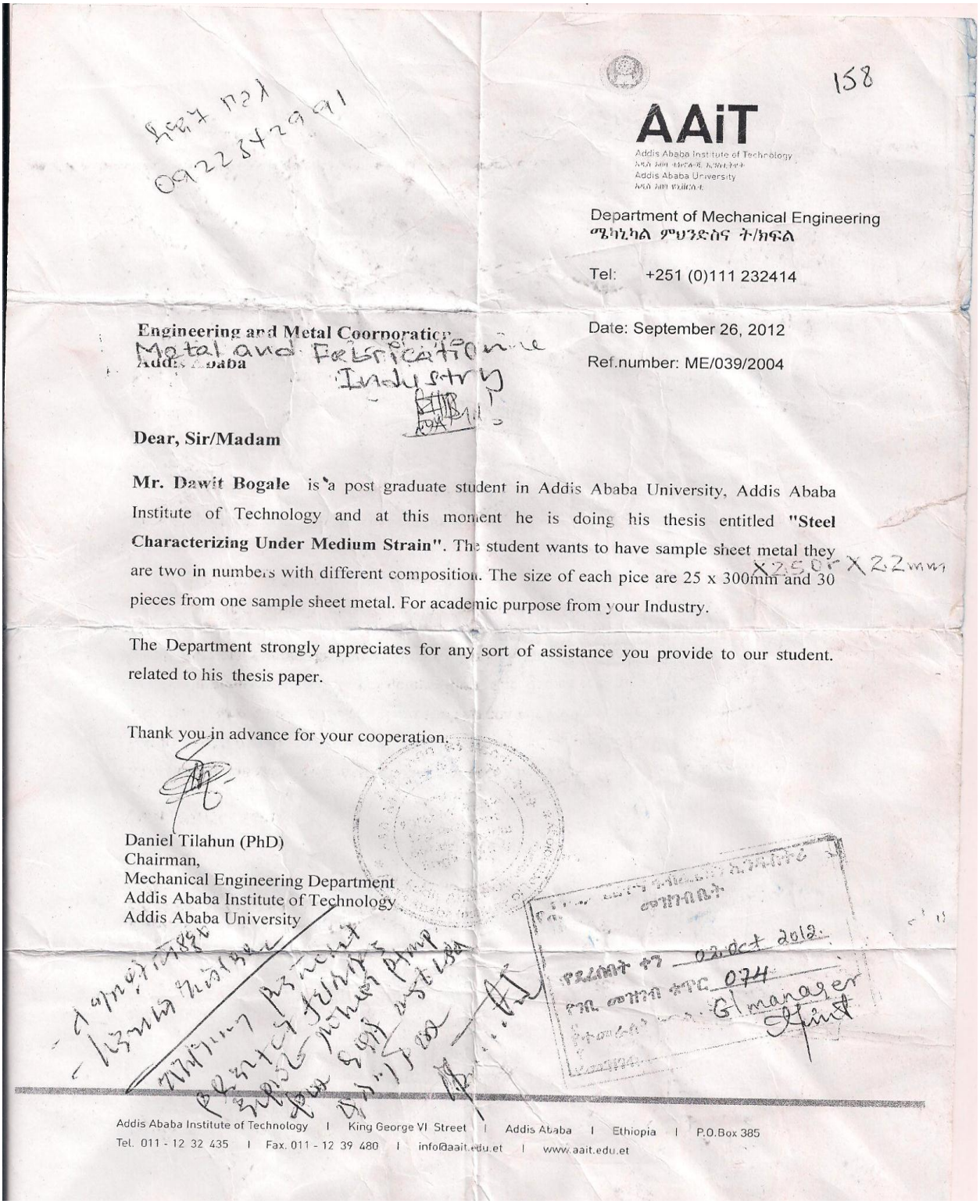

AAiT
Addis Ababa Institute of Technology
Addis Ababa University

158

Department of Mechanical Engineering
ሜካኒካል ምህንድስና ት/ክፍል

Tel: +251 (0)111 232414

Date: September 26, 2012

Ref.number: ME/039/2004

Engineering and Metal Coorporation
Addis Ababa
Metal and Fabrication Industry

Dear, Sir/Madam

Mr. Dawit Bogale is a post graduate student in Addis Ababa University, Addis Ababa Institute of Technology and at this moment he is doing his thesis entitled **"Steel Characterizing Under Medium Strain"**. The student wants to have sample sheet metal they are two in numbers with different composition. The size of each pice are 25 x 300mm and 30 pieces from one sample sheet metal. For academic purpose from your Industry.

X25 or X2.2mm

The Department strongly appreciates for any sort of assistance you provide to our student. related to his thesis paper.

Thank you in advance for your cooperation.

Daniel Tilahun (PhD)
Chairman,
Mechanical Engineering Department
Addis Ababa Institute of Technology
Addis Ababa University

02 Oct 2012
074
G/manager

Addis Ababa Institute of Technology | King George VI Street | Addis Ababa | Ethiopia | P.O.Box 385
Tel. 011 - 12 32 435 | Fax. 011 - 12 39 480 | info@aait.edu.et | www.aait.edu.et

The picture below indicates receipt for article of issuing the shell and mill cutter for the high precision milling machine for the purpose of producing dog bone specimen on the machine

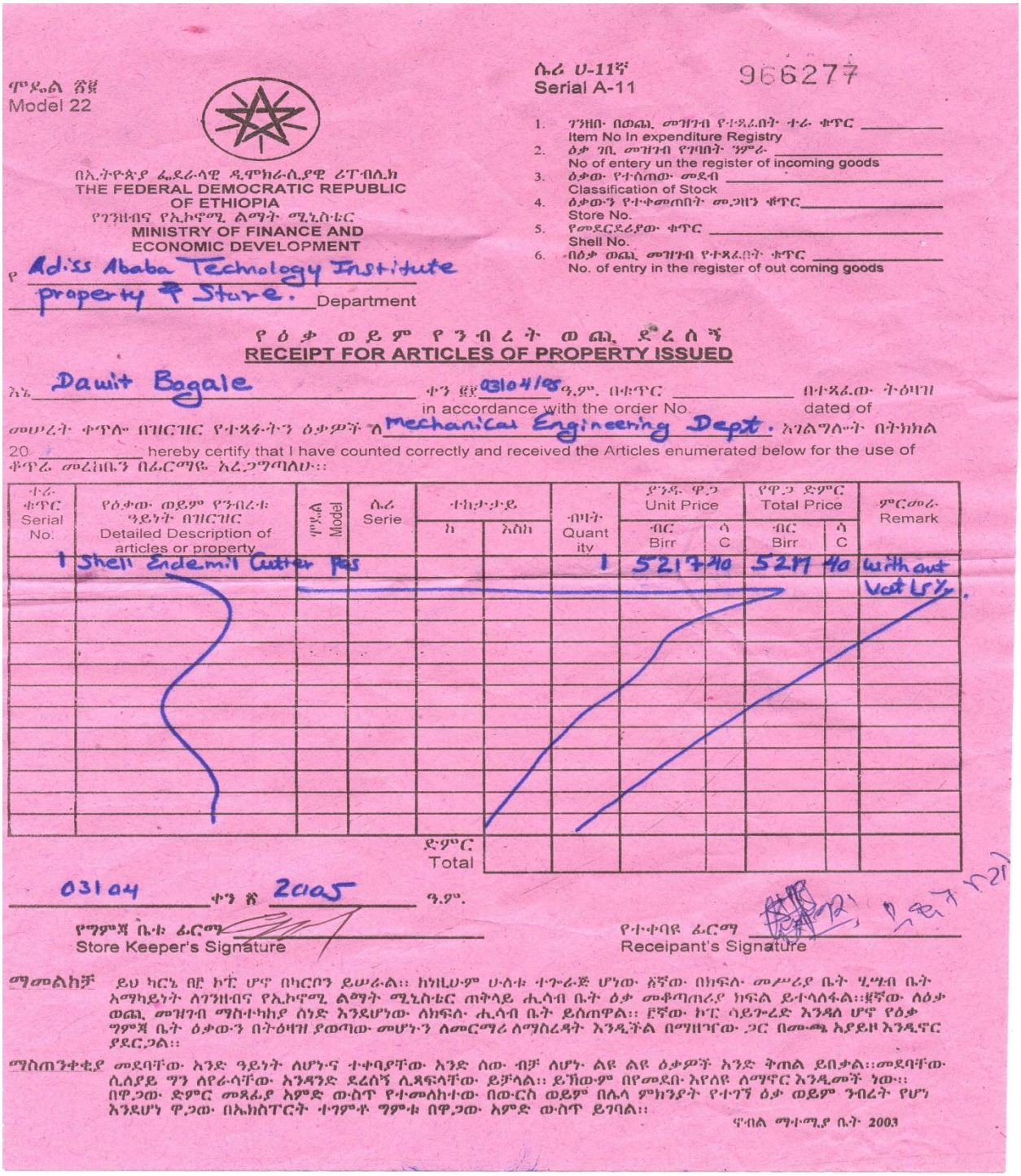

ሞዴል ፳፪
Model 22

ሼሪ ሀ-11ኛ
Serial A-11

966277

1. ገንዘቡ በወጪ መዝገብ የተጻፈበት ተራ ቁጥር _____
Item No in expenditure Registry
2. ዕቃ ገቢ መዝገብ የገባበት ንምራ _____
No of entery un the register of incoming goods
3. ዕቃው የተሰጠው መደብ _____
Classification of Stock
4. ዕቃውን የተቀመጠበት መጋዘን ቁጥር _____
Store No.
5. የመደርደሪያው ቁጥር _____
Shell No.
6. በዕቃ ወጪ መዝገብ የተጻፈበት ቁጥር _____
No. of entry in the register of out coming goods

የኢትዮጵያ ፌደራላዊ ዲሞክራሲያዊ ሪፐብሊክ
THE FEDERAL DEMOCRATIC REPUBLIC OF ETHIOPIA
የገንዘብና የኢኮኖሚ ልማት ሚኒስቴር
MINISTRY OF FINANCE AND ECONOMIC DEVELOPMENT

የ Adiss Ababa Technology Institute property & Store. Department

የዕቃ ወይም የንብረት ወጪ ደረሰኝ
RECEIPT FOR ARTICLES OF PROPERTY ISSUED

አኔ Dawit Bogale ቀን ፪ኛ 03104/05 ዓ.ም. በቁጥር _____ በተጻፈው ትዕዛዝ መሠረት ቁጥሩ በዝርዝር የተጻፉትን ዕቃዎች ለ Mechanical Engineering Dept. አገልግሎት በትክክል
in accordance with the order No. dated of
20 hereby certify that I have counted correctly and received the Articles enumerated below for the use of
ቁጥሬ መረከቤን በፊርማዬ አረጋግጣለሁ።

ተራ ቁጥር Serial No.	የዕቃው ወይም የንብረቱ ዓይነት በዝርዝር Detailed Description of articles or property	ሞዴል Model	ሼሪ Serie	ብዛት Quantity	ያንዱ ዋጋ Unit Price ብር Birr	ሳ C	የዋጋ ድምር Total Price ብር Birr	ሳ C	ምርመራ Remark
1	Shell Endemil Cutter	Yes		1	5217	40	5217	40	without Vat 15%
			ድምር Total						

031 04 ቀን ፳ 2005 ዓ.ም.

የግምጃ ቤቱ ፊርማ _____
Store Keeper's Signature

የተቀባዩ ፊርማ _____
Receipant's Signature

ማመልከቻ ይህ ካርኔ በደ ኦሪ ሆኖ በካርቦን ይሠራል። ከነዚህም ሁለቱ ተጉራጅ ሆነው ፫ኛው በክፍለ መሥሪያ ቤት ሂሣብ ቤት አማካይነት ለገንዘብና የኢኮኖሚ ልማት ሚኒስቴር ጠቅላይ ሒሳብ ቤት ዕቃ መቆጣጠሪያ ክፍል ይተላለፋል።፬ኛው ለዕቃ ወጪ መዝገብ ማስተካከያ ሰነድ እንደሆነው ለክፍለ ሒሳብ ቤት ይሰጠዋል። ፫ኛው ኦሪ ሳይጐረድ እንዳለ ሆኖ የዕቃ ግምጃ ቤት ዕቃውን በትዕዛዝ ያወጣው መሆኑን ለመርማሪ ለማስረዳት እንዲችል በማዘጋጀው ጋር በመጫ አያይዞ እንዲኖር ያደርጋል።

ማስጠንቀቂያ መደባቸው አንድ ዓይነት ለሆኑና ተቀባያቸው አንድ ለው ብቻ ለሆኑ ልዩ ልዩ ዕቃዎች አንድ ቅጠል ይበቃል።መደባቸው ሲለያይ ግን ለየራሳቸው አንዳንድ ደረሰኝ ሊጻፍላቸው ይቻላል። ይኸውም በየመደቡ እየለዩ ለማኖር እንዲመች ነው። በዋጋው ድምር መጻፊያ አምድ ውስጥ የተመለከተው በውርስ ወይም በሌላ ምክንያት የተገኘ ዕቃ ወይም ንብረት የሆነ እንደሆነ ዋጋው በኤክስፐርት ተገምቶ ግምቱ በዋጋው አምድ ውስጥ ይገባል።

ጥብል ማተሚያ ቤት 2003